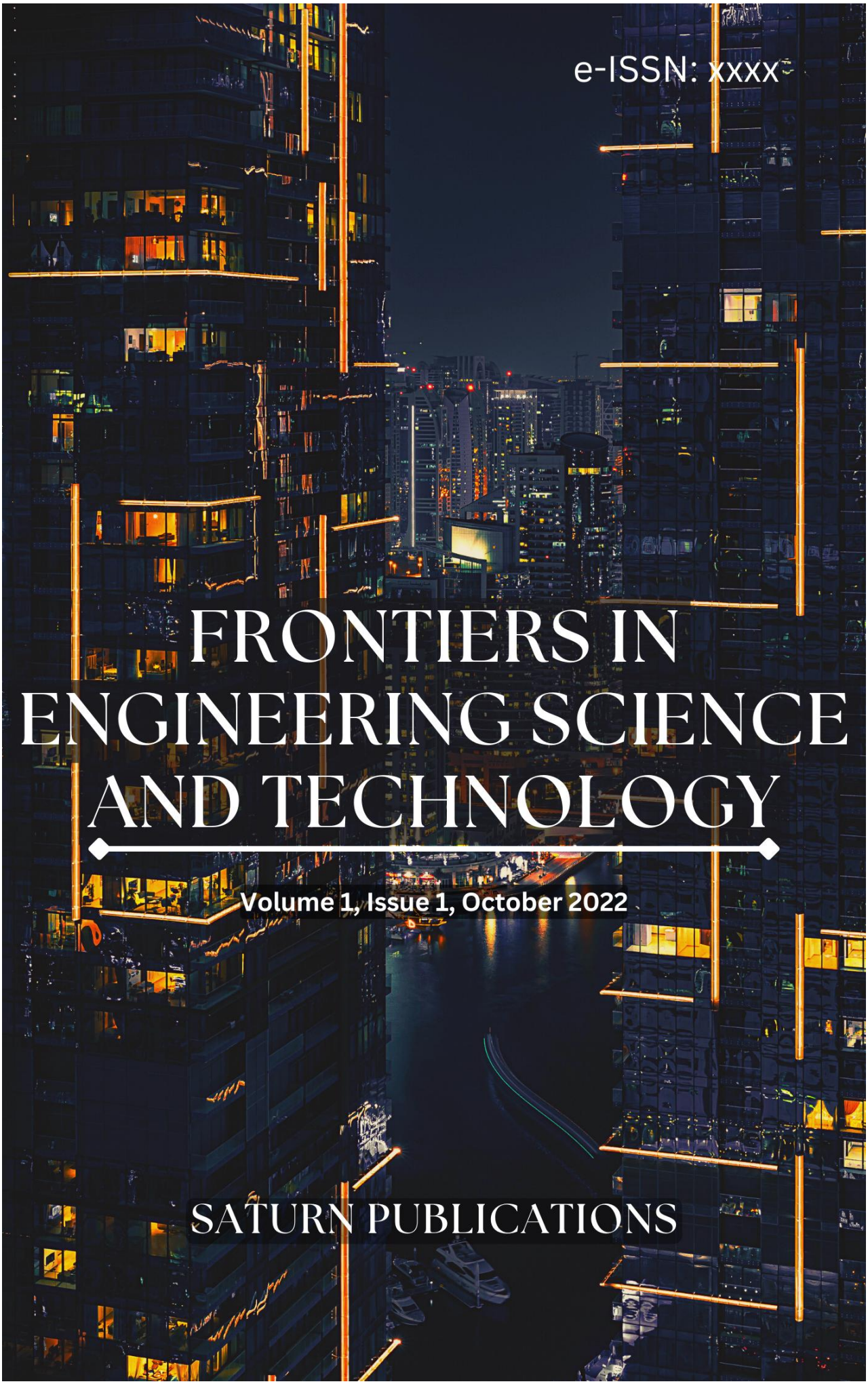

e-ISSN: xxxx

FRONTIERS IN ENGINEERING SCIENCE AND TECHNOLOGY

Volume 1, Issue 1, October 2022

SATURN PUBLICATIONS


SATURN PUBLICATIONS
SP

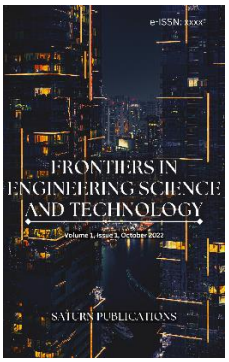

About the Journal

Frontiers in Engineering Science and Technology (FEST) is a peer-reviewed international journal that aims to publish cutting-edge research at the forefront of engineering and technology. Our mission is to advance the understanding and application of fundamental principles in engineering and technology, while also addressing current and emerging challenges facing the field.

The scope of the journal includes all areas of engineering and technology, including but not limited to mechanical, electrical, civil, chemical, aerospace, computer, environmental, industrial, mechanical, telecommunications, and biomedical engineering. We welcome original research papers, review articles, technical notes, and perspectives from researchers, academics, and industry professionals that explore a wide range of topics such as materials science, robotics, renewable energy, nanotechnology, machine learning, and many others.

At Frontiers in Engineering Science and Technology, we are committed to maintaining the highest standards of scientific rigor, transparency, and ethical publishing practices.

Our editorial board comprises leading experts in their respective fields who bring a wealth of knowledge and experience to the journal. We are committed to providing a rigorous peer-review process to ensure that all published articles meet the highest standards of quality and scientific integrity.

FEST is an open-access journal, making all content freely available to readers worldwide. The journal intends to become a leading resource for researchers, practitioners, and students in engineering and technology, promoting collaboration and innovation across disciplines and boundaries.

Frontiers in Engineering Science and Technology (FEST) is published by Saturn Publications, a subsidiary of **Saturn Research and Education Nexus (SMC-Pvt) Ltd.** registered under Section 16 of the Companies Act, 2017, SECP, Pakistan.

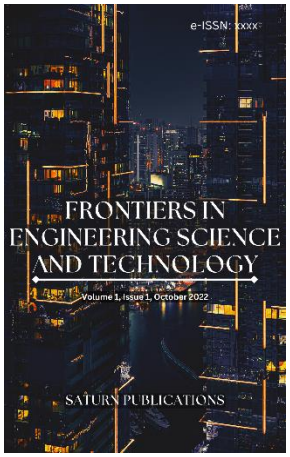

Table of Contents

Saturn Publications

Frontiers in Engineering Science and Technology 1(2022) 2201-2211

www.saturnpublications/fest

IoT Based Smart Battery Monitoring System Using NODEMCU and ThingSpeak

Muhammad Mujtaba Habib[1,*], Abdul Wasiq Siddiqui[2], Syed Muhammad Ibad Ur Rehman[3], and Saqib Hussain[4]

NED University of Engineering & Technology, Karachi, Pakistan

Received 20 April 2022; Accepted 17 September 2022

Abstract

There are many research articles featuring the significance of batteries that require energy stockpiling for some reasons. Lead-Acid batteries are generally utilized in light of their dependability and strength. We chose Lead-Corrosive batteries since they are not difficult to screen and ordinarily accessible in Pakistan. This project will describe the Management System for Lead-Acid batteries, designed to monitor the battery's behavior. In order to accomplish this goal, the following system design objectives were initiated. Lead-Acid batteries are being used because of their increased cost-effectiveness compared to the other type of batteries available in the market all around us, domestically and commercially. They consist of two electrodes—a cathode and an anode—dipped in an electrolytic solution. The battery can withstand numerous charges and recharge cycles, but temperature significantly affects the battery's performance. High and low temperatures can impact the battery heavily in the long and short term. If not properly monitored, the extreme temperature will almost certainly result in battery failures. It would be easier to study the behavior of the battery and predict its lifecycle, charging, and discharging times, so we will deploy a mechanism to automate the log as mentioned above parameters to improve the battery payback period. The objective of this project is to provide different parameters of the lead acid battery, such that DoD (Depth of discharge), SoC (State of Charge), SoH (State of Health), current, voltage, time estimation (charging/discharging), temperature and water level. The project involves designing and developing a battery management System (BMS). It smartly monitors, controls, and manages battery health.

Keywords: Smart Battery Monitoring System; NODEMCU; Battery Health; Battery Management System (BMS).

1. Introduction

Many resources focus on renewable energy, like geothermal, hydro, solar, and wind energy, yet some renewable energy has some restrictions in producing energy. For example, Solar PV cell modules can only generate a limited amount of energy during the scorching sun. Smart microgrids are used to overcome these limitations (García Vera et al., 2019). Battery backups are also needed in smart microgrids when the source is not producing energy.

A systematic battery management system needs to be implemented to monitor the battery's performance continuously. The battery deterioration process should be diminished by molding the battery in an appropriate way by calculating its charging and releasing summary, much under different burden conditions. As a rule, the battery lifetime will be lessened whenever the battery is worked under a broad scope of warm conditions, especially in a high-beat current situation. Batteries are sheltered in spite of reports of blasts or disappointment. A battery monitoring system is required in order to monitor the operating system and performance of any Lead-Acid battery life, such as charge and discharge and many other processes. Battery monitoring system designed to measure device parameters such as battery voltage, current, temperature, mixture solution level, etc. These parameters are allowed to be processed to monitor the two main states related to the health of any battery, the first is a state of charge, and the second is the depth of discharge of the battery. SOC gives the present state of the battery and gives powers to batteries to powerfully be charged and released at that level reasonable for battery life enhancement. In this way, SOC helps in the administration of batteries. The battery monitoring system is required to monitor the operational performances, system, and battery life, such as the discharge and charging process.

Human Machine Interface (HMI), the internet of things (IoT) based Battery Monitoring System, which is developed in this work, consists of a communication channel from and to the IED, data acquisition, Human Machine Interface (HMI). This Battery Management System aims to monitor the basic parameters to help gauge the battery's life and conditions. Incorporating Cloud and IoT into the Battery Management System will help analyze the data in real time. This could be best for the organizations to focus on the company's goals rather than self-monitoring the battery's parameters.

Problems Statement

Lead acid battery life and its usage is a threatening problem in Pakistan; Lead acid batteries are used domestically, commercially, and industrially. As solar energy is used widely, batteries are not monitored; they are usually broken and overused. The payback amount cannot be recovered in batteries. Batteries are hot; they can explode and also affect the charging and discharging cycles which could threaten the overall life of the battery. There's no correct methodology accessible to calculate its parameters.

Moreover, for UPS and solar panels installation, there is a requirement for a battery. According to the research, many electricity users partially and fully adopt renewable resources like solar energy. Most people are unaware of battery management protocols, so there may be issues that they cannot diagnose effectively. As indicated, the electricity shortfall is at its peak in the summer in Pakistan; many domestic users cannot use its power. There are the following fundamental problems:

- **Electrolyte Loss:** The electrolyte deficiency in a Lead acid battery occurs through gassing as hydrogen evades during charging and discharging. Venting causes the electrolyte to become more concentrated. Loss of electrolyte (Battery University, 2010) in Lead acid batteries is a recurring problem that is often caused by overcharging.

- **Sulphation:** Sulphation occurs when a battery is deprived of a full charge; it develops and stays on battery plates. Too much Sulphation can obstruct the chemical to electrical conversion and significantly impact battery performance (Crown Battery, n.d.). When your battery has a development of sulphates. The following can happen:

    - better charging time
    - excessive Temperature rise
    - little running times for charge
    - fully battery failure

- **Stratification:** Stratification occurs during discharge and recharges when the acid in the electrolyte neglects to blend in with the water and settles to the lower part of the battery case. Over time, the concentrated acid at the lower part of the cell can harm the battery plates and fundamentally (Bobby, 2014) diminish the Service life of the battery.

- **Separator Failure:** The initial function of the separator is to block physical contact between the anode and cathode. Separator Failure occurs when there is localized heat up, large-scale heat up, uncontrolled discharge, and penetration of the separator by foreign particles; thus, the separator is no more effective in preventing physical contact between anode and cathode. (Zhang et al., 2017).

In conclusion, while there are a few methods available that are as efficient as the one proposed in this paper, they have not been innovative enough to identify and address the common problems faced in the power sector in Pakistan. Despite the gradual increase in power generation, administrative issues still pose a challenge. The proposed smart lead-acid battery monitoring system provides real-time monitoring of all parameters, unlike other systems that calculate them at once. Moreover, it allows users to access data anytime and anywhere, making it suitable for both domestic and commercial use in stabilizing the electrical shortfall in Pakistan.

2. Objectives

- Modeling of battery system using sensors.
- Programing of battery monitoring system using NodeMCU.
- Measuring the various parameters of the battery such as DOD (Depth of discharge), SoC (State of charge), maximum current and voltage, time estimation, acid temperature, and water level.
- Monitoring all the data with the help of ThingSpeak to aggregate, visualize, and analyze live data streams in the cloud.

3. Scope and Limitations

Lead acid batteries are made from abundant, low-cost materials and nonflammable water-based electrolyte that significantly minimizes environmental impact. Nevertheless, forecasts of the downfall of Lead acid batteries have focused on the health effects of lead. A large gap in technological progressions should be seen as an opportunity for scientific engagement to extensively diversify Lead acid batteries into power grid applications which currently lack a single energy storage technology with optimal technical and economic performance ("Forbes Search"), Lead acid batteries are widely used in our industries, markets, homes, etc., Solar energy is the cheap form of electricity, but it has its own demerits that it cannot produce electricity without solar radiations hence to compensate the issue there will be a need of a battery that can store enough solar energy for consumption in the absence of solar radiations. We need to monitor (EHS – Concordia, 2016) the parameters of the batteries that will help us maintain the battery, prolong the battery's lifetime, and save costs.

4. Significance

A quintessential design of the smart lead acid battery can facilitate its consumers as well as companies. The smart lead acid battery can track data of different parameters, and a user can check it anywhere in the world. The smart lead acid battery reduces human involvement in maintenance work. Commercializing the smart lead acid battery type is a step toward digitalizing the electrical power sector in Pakistan. The main advantages of the lead–acid battery (EHS – Concordia, 2016), are that it is a cheap power source, is almost fully recyclable, and is safe equipment.

5. Literature Review

Batteries are the most widely recognized electrical energy storage gadgets. Various academic projects revolve around the Lead Acid Battery. Lead-Acid batteries are being used because of their cost-affectivity as compared to the other type of batteries available in the market (EHS – Concordia, 2016), all around us domestically and commercially. It is important to monitor the status of the battery and the other important parameters which can reduce the life of a battery. For this purpose, we read some research papers to learn how we will implement this in our project. We have taken help from YouTube to compare the sensors which we are using in our project for reliability and low cost. The followings are the important parameters:

- Temperature
- Water level
- State of charge, discharge, and health

For connecting each parameter, we have used Node MCU (ESP 32 module), which consists of 30 total pins and 12 Analog input pins, which is further connected with ThingSpeak, which is an IoT platform it collects data in the cloud ("ESP32 DevKitC Pinout," 2021) and analyzes and acts according to the given instructions.

Temperature of the Battery

The temperature has a major effect on the battery and its performance. High and low temperatures can impact the battery in the long and short run. If not properly monitored, extreme temperatures will almost certainly result in battery failures (Hutchinson, 2004). We picked up PT-100 (platinum-100) of three wires for temperature monitoring. The PT-100 of two wires has less accuracy (Process Parameters, 2019), which is why we have used the PT-100 of three wires, as we require high accuracy. Faults in a battery occur due to the connected circuit, which creates an impact on the battery's temperature (in degrees). Some of the common faults that cause in increasing the battery's temperature are poor ventilation, shorted cells, ground faults, and lost regulation of charging. To check the battery temperature ("How does a Pt100 sensor work?", n.d.), recognize a portion of these faults. Super-durable harm can happen if the battery temperature is not observed and appropriately controlled. In the best-case scenario, some mechanical mutilation or change in the synthetic arrangement will occur, bringing about an expensive battery replacement (Akcp.com). At most exceedingly terrible, the battery cell can detonate, spill synthetics, or cause a fire that could be amazingly destructive to the climate.

The other reason we choose this sensor is that it is waterproof and can work in the acidic nature of water. The size of the sensor is such that it can be used in batteries easily. It is also being used in the industry for temperature monitoring.

Other temperature measurement sensors are available in the market, such as thermistors, thermocouples, and RTDs. The comparison of the YouTube videos shows that RTD gives the most accurate results. RTD slightly has the disadvantage of the cost as it is expensive compared to other temperature sensors. But we have neglected this factor to increase the reliability of our sensor (Resistance thermometer, n.d.)

CRITERIA	RTD	THERMOCOUPLE	THERMISTOR
Sensing range	(-260 to 850)°C	(-270 to 1800)°C	(-80 to 150)°C
Accuracy	±0.01°C	±0.5°C	±0.1°C
Linearity	Best	Good	Worst
Stability	Best	Low	Moderate
Sensitivity	Moderate	Low	Best
Cost	(1100 to 1400)Rs	(600 to 1200)Rs	(1100 to 1500)Rs
Specifically for	High accuracy	High temperature	Point sensing

Table. 1. Comparison between temperature sensors

The above parameters target the performance of the temperature sensor, and according to all the research papers, we found that the RTD is the best fit for temperature sensing you can see clearly from the above table of comparison. Planar obstruction temperature locator, RTD, can be produced with microelectronics preparing methods. In any case, the fabricated planar resistor requires an additional progression for change of the 0degC reference opposition, R 0. In this paper, we have assessed the creation of nickel-RTD transducers for shrewd temperature sensors. The obstruction change step is avoided by applying the brilliant sensor idea, as the alignment bend can be put away in the Transducer Electronics Datasheet (TEDS). The RTDs have been manufactured by warm dissipation of nickel onto an alumina substrate. Alignment bends have been estimated as an element of temperature, and high linearity is noticed. Two unique models for molding and handling gadgets are examined.

A thermocouple is a temperature-estimating gadget comprising two disparate conductors that reach each other in at least one spot, where a temperature differential is capable by the various conductors (or semiconductors) (Pandya, 2016). It creates a voltage when the temperature of one of the spots contrasts with the reference temperature at different circuit pieces. Thermocouples are a generally utilized sort of temperature sensor for estimation and control (O'Grady, 2019). The primary impediment with thermocouples is exactness; framework mistakes short of what one degree Celsius (°C) can be hard to accomplish.

Water Level of The Battery

Water-level of the battery is one of the most important parameters of the battery because the low water level of the battery will make the solution more acidic that will cause the cell of the battery to be damaged, and it will reduce the charging capacity of the battery ("Battery basics", 2020) For this purpose; we have used an Ultrasonic sensor (HSSR04) (Lastminuteengineers.com. High-

frequency sound (ultrasound) waves are generated by an ultrasonic sensor. Echo is reflected when the ultrasound wave hits the object which is sensed by the receiver. It is usually used to determine the distance of the objects. The ultrasonic sensors are easy to use and not hazardous during operation for nearby objects, persons, equipment, or material. We learned that HS-SR04 is used widely for academic projects by searching the internet. Radar sensors are the best sensors in the market. Still, they are costlier than the ultrasonic sensor and partially available in the market, so that is why we picked up HS-SR04 to monitor the water level of the battery (Dahl, 2013).

PARAMETERS	INFRARED SENSOR	ULTRASONIC	RADAR SENSOR
Range	(10 -80) cm	(2-10) cm	(100) m
Beam width	75^0 C	30^0 C	15^0 C
Frequency	353THz	40KHz	80GHZ
Unit cost	1500pkr	300pkr	2500pkr

Table. 2. Comparison between water level sensors

Depth of Discharge of the Battery

The depth of discharge of the battery is an important parameter. Depth of discharge means the fraction or percentage available from the fully charged battery. By monitoring it, we can calculate the battery cycle. And also, as the fast discharge of the battery causes the capacity of the battery to reduce, so by monitoring it, we can save the battery from being fast discharged. By taking help from the website, we see that if the depth of discharge is 20%, it can give 4000 cycles, and similarly, if the depth of discharge is 50% and 100%, it will give 1600 and 800 cycles, respectively. So, we can conclude from this why it is important to monitor the depth of discharge of the battery ("Characteristics of lead-acid batteries", n.d.)

State of Charge of the Battery

The state of charge (SOC) represents the current capacity of any battery. The state of charge acts like a fuel gauge in any vehicle. It lets users know how long they can operate the load or machine before it runs out of energy. The quick charging of the battery can cause a decrease in the battery's lifetime, and also it affects the cells of the battery. Fast charging of the battery can also cause the temperature of the battery to be increased. Many methods can estimate the state of charge; the first is coulomb counting, which is the quickest and easiest method. So, you have only to calculate what percentage capacity (Ah) you took from the battery during a period of your time (it doesn't matter if it's variable or not) (Chang, 2013).

Battery State Calculation

The battery position is utilized as an information variable for the electrical administration, and moreover, it is a significant variable for the client. So, the battery condition may be utilized to gauge the crossing over time or the normal lifespan of the battery. The condition of the battery may be improved, portrayed by the accompanying two variables: SOC and DOD both variables are not autonomous and impact the battery execution (for example, accessible limit). The relationship has appeared in SOC assurance much of the time Ah checking, including charge misfortune estimation, is used (Yao & You, 2020). Two or three good working strategies are known and utilized for SOH assurance. It relies firmly upon battery innovation, and the sort of use which strategy is useable shows a technique utilizing an ideal channel calculation for SOC and SOH assurance (Chiasson et al., 2003). Different strategies like fluffy, bunching, and neural systems were additionally evolved and tried.

Microcontroller (NODEMCU ESP-32)

We have used NODE MCU ESP-32 instead of another micro-controller chip to extract our information from the sensors and show the result on the result window or screen (Veit & Johra, 2021). By comparing it with another microcontroller like Arduino, we found that Arduino doesn't have a Wi-Fi chip built-in, we can add an external Wi-Fi module ("The Internet of Things with ESP32", n.d.), but it will increase the complexity of the circuit Arduino was originally made for the professional users. At the same time, the ESP32 module is done for DIY projects because it is easy to use, and the most critical factor is its cheaper than Arduino. There are products with ESP32 and ESP8266 inside. And it also doesn't have more analog pins as we required, so by looking at all of these things, we have chosen NODE MCU ESP-32. There are also other models of NODE MCU ("NodeMCU ESP32", n.d.), like ESP-8266; we have considered ESP-32 because ESP-8266 has only one analog input pin. It will link our information from the screen to the cloud. For this purpose, we are using ThingSpeak, which will show the parameters information of the battery on the cloud or on a website that can be accessed from anywhere and at any time (Kumar et al., 2020)

CRITERIA	ESP32	ESP8266	AURDUNIO UNO	RASPBERRY PI
Core count	Single/dual-core	Single-core	Single-core	Dual-core
Arquitetura	32 BITS	32 BITS	32 BITS	32BITS
Clock	160MHz	80MHz	16MHz	133kHz
Wi-Fi	Built- in	Built-in	Not supported	Not supported
Ram	512KB	160Kb	2Kb	264kb
Gpio	36	17	14	26
Adc	18	1	6	3
Dac	2	0	0	0
Mcu voltage	3.3VDC	3.3 VDC	5VDC	3.3VDC

Table. 3. Comparison between microcontrollers

Internet of Things (ThingSpeak Platform)

The ThingSpeak platform is a service that provides IoT analytics capabilities. We have utilized this platform due to

its ability to store data in the cloud, analyze and visualize it, and act upon given instructions. By using this software, we are able to instantly visualize data collected by devices on ThingSpeak, such as the ESP8266 daily task (2018).

IoT devices and sensors have the potential to manage a network of physical objects and can provide observations across multiple layers of the network and infrastructure utilized by customers. With the help of data hardware version, code version, and location, one can collect information beyond what can be obtained from an on-site monitor alone. It is important to look beyond just the sensor data and consider how the data is captured and transferred, including timestamps and error logs, in order to enhance network performance (The role of cloud computing, n.d.).

PCB Designing and Dip Trace

For our circuit planning and carrying out the reason, we have utilized PCB (printed circuit board). First and foremost, we were attempting to carry out the hardware in Vero board; however, it has some marginal inconveniences, so to ad-lib our work as suggested by (Agarwal, 2017), we need to embrace PCB, yet it was a simple assignment at all it is on the grounds that we need to plan our PCB format on a product. Likewise, the disarray became which is to choose which programming we picked for our plan. We have analyzed a lot of programming; however, the interface of the plunge follows was intriguing and simple to utilize ("Dip Trace", n.d.). We have seen numerous recordings of the plunge following and working on the PCB plan on YouTube (Hamilton, 2013).

*Liquid Crystal Display (LCD 20*4)*

There are 20 characters for each line and 4 such lines in a 20x4 LCD. Each character is shown in a 5x7 pixel grid in the LCD. There are two registers in this LCD, Command, and Data. This is a standard HD44780 regulator LCD. I2C Module has an inbuilt PCF8574 I2C chip that changes I2C sequential information to resemble information for the LCD show. These modules are, as of now, provided with a default I2C address of either 0x27 or 0x3F. To figure out which adaptation you have, check the black I2C connector board on the underside of the module.

Efficiency of Battery

Battery efficiency is the measure of energy you can get out of a battery relative to the amount of energy that is put into the Lead-Acid battery is not always 100% at storing electricity - you may by no means get out as tons as you install while charging. Overall, a performance stage of 85% is frequently assumed. The performance will depend upon different factors; however, we are mainly focusing on the charging or discharging of the temperature. The better the charge of fee or discharge, the decrease in the performance of the battery. The country of fee of the battery will likewise have an impact on fee effectiveness. With the battery at ½ of the fee or less, the fee performance can be over 90%, losing closer to 60% while the battery is above 80% charged. However, it has been observed that if a battery is best partly charged, performance can be decreased with every fee. If this case persists (the batteries by no means attaining complete fee), the battery's life can be reduced.

In this project, we are trying to monitor SOC, SOD, and temperature with immediate effect with rightly distributed intervals and the intensity from under controlled situation to the alarming situation; we are incorporating buzzers and lead for effective human interactive indications; hence we can counter the problems earlier, and by this way, we can ensure prolong battery's life and efficiency.

Temperature	Life of the battery with monitoring(Years)	Life of battery without monitoring(Years)	Comments
25*C	8<x<12	5<x<9	Optimum Temperature of the battery
33*C	4<x<6	2.5<x<4.5	Should be monitored by sensors
41*C	2<x<3	1.25<x<2.25	This indicates there is a fault in battery
49*C	1<x<1.5	x< 1 year	Battery should be replaced

Table 4. Life of batteries with and without monitoring

Human Machine Interface

HMI is used in ventures and forces plants to control and screen machines. An exceptionally normal HMI that you frequently experience is ATM. It is hard to have a nice, robotized measure in organizations without an HMI; usually, HMI is in a sort of screen like a PC contact screen. It tends to be put in charge boards where the Maintenance faculty can work without much of a stretch work and screen it. HMI shows different boundaries on screen at a time, where it can show an extremely exact degree of temperature, water level, and the ostensible voltage of the battery. The engineering professional has to design each parameter and do the coding parts; we only can utilize it where a large need of batteries is required to become economical for the overall production.

The GLG Toolkit incorporates the GLG Graphics Builder - a graphical editorial manager with a point and snaps interface for making dynamic HMI and SCADA screens and charts. With the Graphics Builder, engineers can make elaborate interaction control and framework observing drawings, characterize dynamic conduct, and append continuous information sources. Various pre-assembled parts and ranges are accessible as building blocks in the Builder. A discretionary GIS Map part is additionally accessible.

Block Diagram

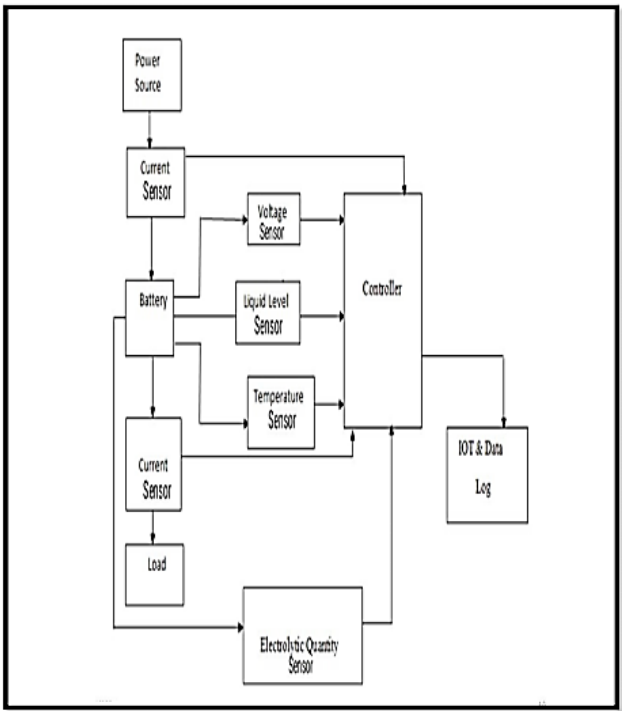

Fig. 1. Block Diagram

6. Methods

Gathering information from the literature review and utilizing the PT100 RTD temperature sensor, we have created a circuit diagram to connect it to the NodeMCU (esp-32). Secondly, a circuit diagram was drawn on Dip Trace software to obtain the schematic diagram, which was then converted into a PCB design for routing and printing. The third step consisted of imprinting. the PCB design onto the PCB board, drilling the holes, inserting the components, and then soldering them to the board. Our next task was to acquire data through the Arduino IDE, connecting the circuitry to the NodeMCU and programming it accordingly. After the PT100 measured the battery's temperature, we observed the increment in temperature. The objective flow diagram of our process is given as follows:

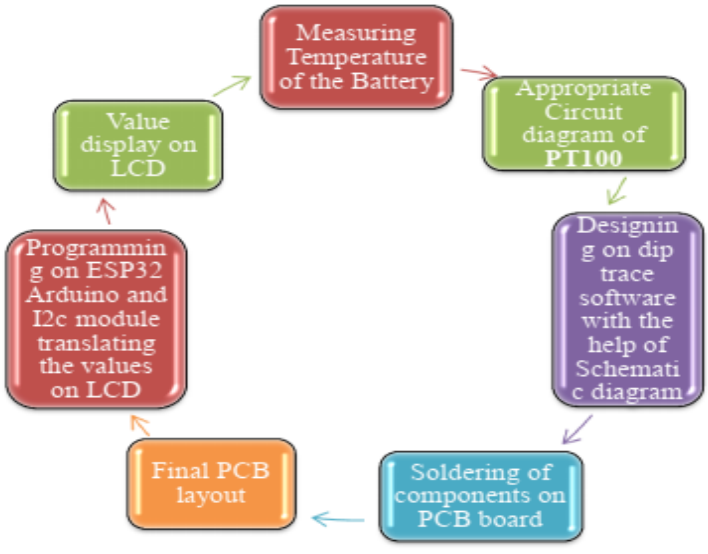

Fig. 2. Process Flow Chart

Circuit Diagram

Creating a circuit diagram to connect the PT100 (RTD) temperature sensor to the NodeMCU (EPS-32) to enable digital visualization of the analog data is necessary. Using the necessary components, the circuit can be designed to connect the sensor and NodeMCU.

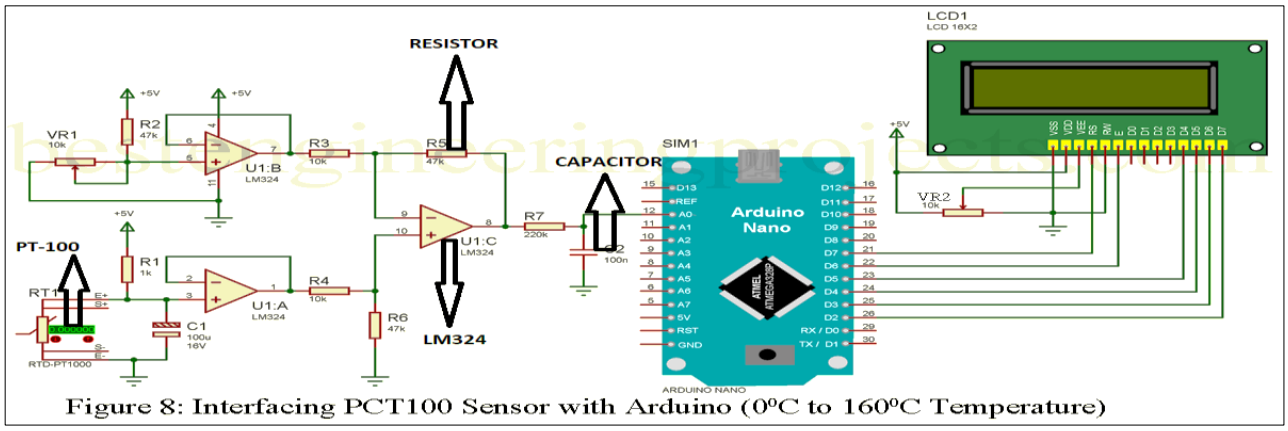

Figure 8: Interfacing PCT100 Sensor with Arduino (0°C to 160°C Temperature)

Fig. 3. Modelled Test System

Measuring the Acid Level of the Battery

Measuring a battery's acid level requires using an ultrasonic sensor, such as the HCSR04. Table 2 of the literature review shows that this sensor is the most suitable for our project due to its size and cost. The ultrasonic sensor works by sending out a sound wave at a frequency above the range of human hearing. The sensor's transducer acts as a microphone to receive and send the sound signal. The four pins of the HCSR04 (ground, trigger, VCC, and echo) are connected to the Node MCU through jumper wires to digitally represent its results on the screen, allowing the user to monitor the acid level of the battery easily.

Measuring The State of Charge of The Battery

The State of Charge is the third most essential metric (SoC). The percentage of a battery's rated capacity is known as the SOC. In other words, SOC is the ratio of the energy saved in the battery to the entire amount of energy that can be saved. If the rated capacity is expressed in coulombs or Ah, the RC should also be calculated in those units. SOC can be calculated using the energy storage capacity when the remaining or rated energy content is measured in watt-hours. The SOC indicates the battery's present state and allows it to be charged and drained safely at a level that extends its life. The battery becomes less efficient as the temperature rises, and the cells become damaged. SoC gives the user access to functionality that isn't present in the battery or that might be required in a fully negative feedback circuit to ensure optimal charging control. There are multiple estimation methods SoC; the first is coulomb counting, Which is the quickest and most straightforward method. So, all you have to do now is figure out what percentage capacity (Ah) you drained from the battery over a while (varying or not).

Measuring the Depth of Discharge of the Battery

A battery's depth of discharge (DOD) defines the charge remaining in the battery. Depth of Discharge can be stated as the ratio between the capacity that is discharged from a fully charged battery and the total battery capacity. The DOD is expressed in percentage. This is because each battery always provides more volts when the battery is 100% charged and low voltage when the battery is empty. A fully charged 12-volt lead-acid battery usually provides 12.7V power. If the lead-acid battery is only 20% left, it will only deliver 11.6V. The batteries we used in the voltage range have lower electrical power than lithium-ion batteries (HAbdi et al., 2017). The life cycle is the number of charge/discharge cycles that any battery can maintain in its useful life. If you regularly discharge batteries at a lower percentage, there will be more efficient cycles than when you discharge the battery to its higher DOD. A standard lead-acid battery offers 200 to 300 discharge cycles ("What is Depth of Discharge", 2020).

The second thing that affects an acid-powered battery's useful life is how you look at it. Batteries in a tropical area (above 30 degrees C) may be extremely hot, reducing the overall battery life. Extremely cold temperatures also have a negative effect on the battery, as it has to work hard and have a high charging capacity. So the conclusion of the above statement is to place batteries at room temperature to help maximize the useful life of the Lead-Acid battery.

Measuring Voltage of the Battery

Voltage in any battery is defined as one of the most important parameters for monitoring. It tells the user that any cell of the battery is getting damaged, and it will cause the other cells of the battery to be damaged as the cells of the lead-acid batteries are connected in series; other if anyone cell gets damaged, it will cause the other cells of the battery to be damaged too and it led the battery to lose its capacity of storing electricity. Every battery comes with a certain voltage and capacity rating. There are cells inside each battery that are connected in series to create voltage levels, and that battery-rated voltage is the nominal voltage at which the battery is supposed to operate. The unit for measuring battery capacity is ampere-hour, denoted as

(Ah). The energy capacity is the battery rated voltage in volts (v) multiplied by battery capacity in ampere-hours resulting in total battery energy capacity in watt-hours.

7. Results

Temperature of the Battery

The result shows the temperature variation given by the heating material by us to ensure that the PT-100 sensor is working perfectly or not. It provides the temperature in (0C).

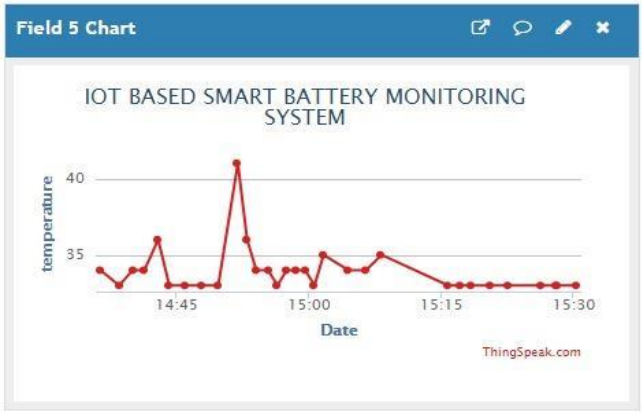

Fig. 4. Temperature of the battery

Liquid Level of the Battery

The demonstration gives the result of our ultrasonic sensors; here, we do the same job as before to ensure the proper working of the sensor. We move our sensor up and down with the reference ground to check it.

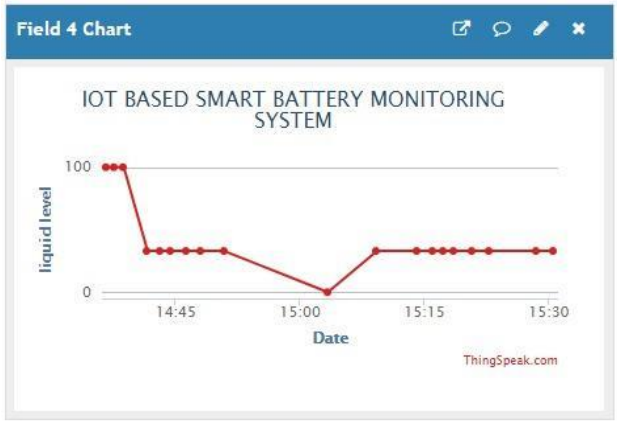

Fig. 5. Liquid level of the battery

State of Charge of the Battery

Here SOC means the state of charge where the graphical reading determines the charging of a battery with charging current provided by the power bang. The below battery is slightly aged, so the results vary, but you can see from this figure that the SOC graph increases with the charger's increase, and the SOC decreases with the increase in time due to the load.

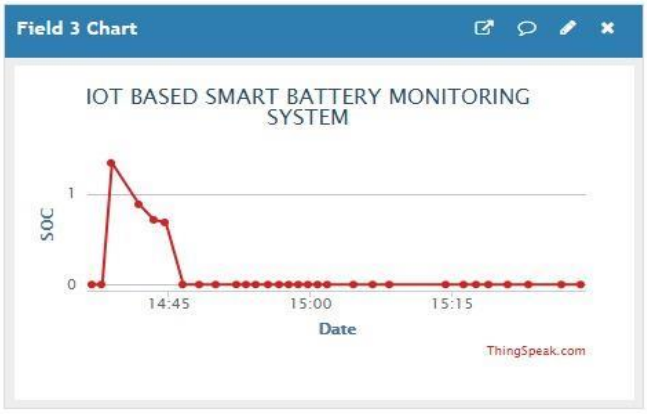

Fig. 6. State of charge of the battery

Depth Of Discharge of the Battery

DOD forms this figure varying because of the change of the loads [note: here we have used filament bulb and light stick as a load to observe the behavior of the DOD of our battery]. And it is totally the opposite of the above-stated SOC.

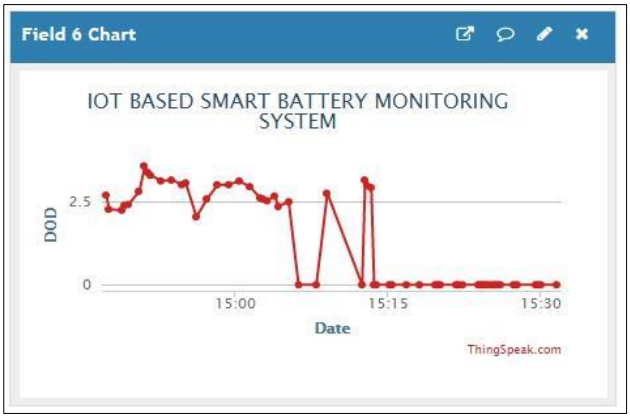

Fig. 7. Depth of discharge of the battery

Voltage of the Battery

The voltage here revolves around the 12v analog values, which you can refer to in Appendix B (Battery specification). We have programmed it to take some average values of the battery and display them on LCD.

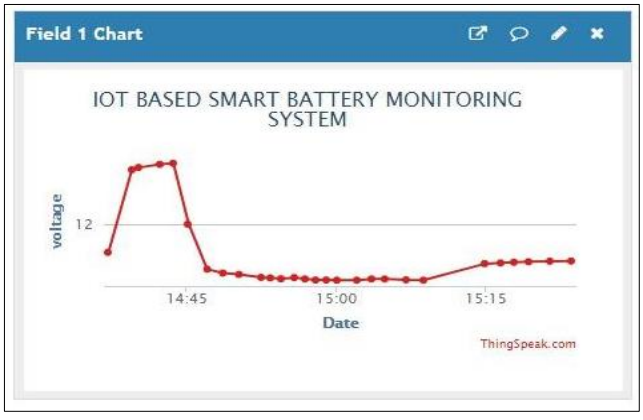

Fig. 8. Voltage of the battery

Battery Percentage

The below result shows how much the battery is charged.

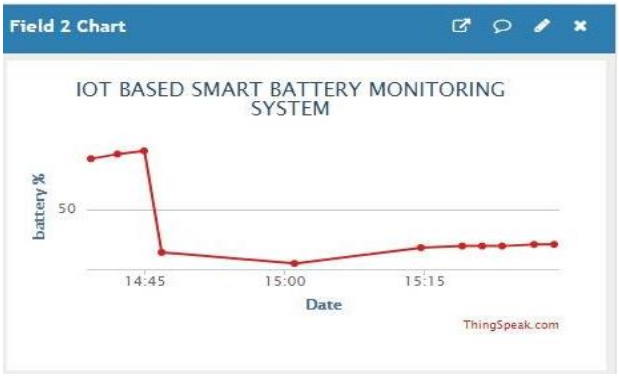

Fig. 9. Battery charging discharging percentage

All Parameters of the Battery

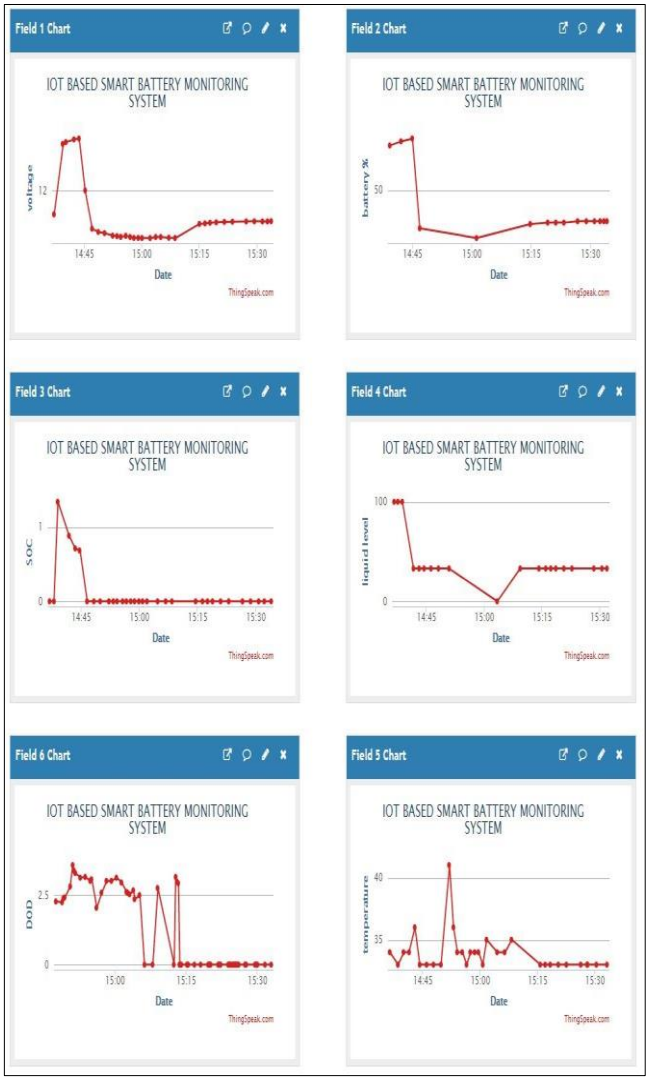

Fig. 10. All parameters of the battery

8. Conclusion

(IoT-based smart battery monitoring system using NodeMCU and ThingSpeak) the intent to provide a much-protected atmosphere around the battery, which can help in having a battery. Therefore, it becomes essential for the detection of basic problems like Electrolyte Loss, Sulphation, Stratification, Separator Failure, and many others; now we have to counter these problems, so we implemented objectives as follows DOD (Depth of discharge), SoC (State of charge), maximum current and voltage, time estimation and acid's temperature and water level. To solve the above-stated problems, we have found a solution. If we consider Pakistan's high demand for battery monitoring systems, it is BMS. In our BMS, we incorporate all the factors that can be hazardous for human life or the environment. We used a temperature sensor (PT-100 three wired), and an ultrasonic sensor (HCSR04), to measure the state of charge, depth of discharge, and the battery's nominal voltage. But to convert it to a single monitoring system, we choose PCB, in which we select dip trace software because of its easy interface and configurations. It is free software best for academic work. Now, we have used ESP 32 microcontroller; to conclude all the above parameters result in a single platform, we select ThingSpeak; it is an IoT-based software used to aggregate, envision, and investigate live information streams in the cloud. We likewise empower putting away these values in the cloud, with the goal that it tends to be recovered later for investigation and can be seen whenever on our cell phone.

9. Future Recommendations

Battery Cell Damage

Subsequently carrying out this proposed idea, we realized that there is further room for modifications in IoT-based smart battery monitoring systems. In the future, it very well may be useful to recognize the specific cell harmed substitution due to if any one cell is harmed, it will cause the whole battery to be squandered. We can do this by observing the voltages of every battery cell, and by noticing the voltage of the cell, we can ensure what cell there is a voltage drop, and the cell is getting harmed; by replacing it, we can make our battery keep going long as the cells in the battery are in series with one another so that if one cell gets harm, its effect can create the other cell can harm as well.

GSM Module

Utilizing a GSM Modem, we can gather this raw information and send it as an SMS message to cell phones. With the assistance of cell phones, information can be gathered and seen even from distant areas where Internet association is powerless. This model can likewise be stretched out for different battery observing frameworks. We likewise empower putting away these values in the cloud, so they very well may be recovered later for investigation and can be seen whenever on our cell phone.

Additionally, by using the GSM (Global System for Mobile Communications) module, we can free our battery from any Wi-Fi relationship in the region as GSM (Global System for Mobile Communications) module can give the

organization associated with it. The disadvantage with the GSM is that we need to make it PTA embraced to get it into the working condition in Pakistan. The cost of the Initial License Fee from PTA support is about PKR 5000 for each module, and Annual License Fee is around 1.5% of yearly gross income with the exception of where a ban is allowed ("Fee Schedule.", n.d.). Regardless, in the wake of getting it upheld from the PTA we can enjoy many benefits.

Human Machine Interface (HMI)

We use HMI in industries and power plants to control and monitor machines. A very common HMI that you often encounter is ATM. It is difficult to have a decent robotized measure in businesses without an HMI. Ordinarily, HMI is in a type of screen similar to a PC contact screen. It can be placed in control panels where the Maintenance personnel can easily operate and monitor it.

HMI shows various parameters on screen at a time, showing a very precise temperature, water level, and the battery's nominal voltage. From this, you can easily analyze the data and make appropriate decisions. They can even connect to the PLCs to exclude laptop use. HMI consists of two main parts: an operation panel and a monitoring screen (Friansa et al., 2017), but it's not easy as you think; firstly, the engineering profession has to design each parameter and do the coding parts we only can utilize it where the large need of batteries are required to become economical for the overall production.

10. References

1. Agarwal, T., "What are the advantages of using A printed circuit board (PCB)," (2017). [Online]. Edgefx.in, Available: https://www.edgefx.in/advantagesusing-printed-circuit-board-pcb/. [Accessed: 09-Sep-2021].
2. Akcp.com. [Online]. Available: https://www.akcp.com/blog/batterytemperature-monitoring-system/. [Accessed: 09-Sep-2021].
3. Battery University, "BU-803c: Loss of electrolyte," Batteryuniversity.com, (2010). [Online]. Available: https://batteryuniversity.com/article/bu-803c-loss-ofelectrolyte. [Accessed: 09-Sep-2021].
4. Bobby, "Understanding acid stratification in lead acid batteries - news about energy storage, batteries, climate change, and the environment," Upsbatterycenter.com, 29-May-2014. [Online]. Available: https://www.upsbatterycenter.com/blog/understanding-acid-stratification-lead-acidbatteries/. [Accessed: 09-Sep-2021].
5. Chang, W. Y. (2013). The state of charge estimating methods for battery: A review. International Scholarly Research Notices, 2013.
6. Chiasson, J., & Vairamohan, B. (2003, June). Estimating the state of charge of a battery. In Proceedings of the 2003 American Control Conference, 2003. (Vol. 4, pp. 2863-2868). IEEE.
7. Crown Battery, "What is a sulfated battery and how to prevent it," Crownbattery.com. [Online]. Available: https://www.crownbattery.com/news/sulfation-and-battery-maintenance. [Accessed: 09-Sep-2021].
8. Dahl, Ø. (2009). High-precision beamforming with UWB impulse radar (Master's thesis).
9. EHS – Concordia. (2016). Lead Acid Batteries. Retrieved February 27, 2021, from Concordia.ca
10. ESP32 DevKitC Pinout, Overview, Features & Datasheet. (2021). In Components101.com. [Online]. Available: https://components101.com/microcontrollers/esp32-devkitc [Accessed: September 9, 2021].
11. Friansa, Koko & Nashirul Haq, Irsyad & Santi, Maria & Kurniadi, Deddy & Leksono, Edi & Yuliarto, Brian. (2017). Development of Battery Monitoring System in Smart Microgrid Based on the Internet of Things (IoT). Procedia Engineering. 170. 482-487. 10.1016/j.proeng.2017.03.077.
12. García Vera, Y. E., Dufo-López, R., & Bernal-Agustín, J. L. (2019). Energy management in microgrids with renewable energy sources: A literature review. Applied Sciences, 9(18), 3854.
13. HAbdi, B., Mohammadi-ivatloo, S., Javadi, A., Khodaei, A. R., & Dehnavi, E. (2017). Energy Storage Systems. In Distributed Generation Systems (pp. 333-368). Elsevier. https://doi.org/10.1016/B978-0-08-100592-6.00010-3
14. Hamilton, C. (2013). A guide to printed circuit board design. Elsevier.
15. Hutchinson, R. (2004). Temperature effects on sealed lead acid batteries and charging techniques to prolong cycle life (No. SAND2004-3149). Sandia National Laboratories (SNL), Albuquerque, NM, and Livermore, CA (United States). Resistance thermometer Pt100 or Pt1000 - WIKA, Wika.com. [Online]. Available: https://www.wika.com/en-en/lp_pt100_pt1000.WIKA
16. Kumar, S., Sharma, K., Raj, G., Datta, D., & Ghosh, A. (2020, February). Arduino and ESP32-CAM-based automatic touchless attendance system. In Proceedings of the 3rd International Conference on Communication, Devices and Computing: ICCDC 2021 (pp. 135-144). Singapore: Springer Singapore.
17. Lastminuteengineers.com. [Online]. Available: https://lastminuteengineers.com/arduino-sr04-ultrasonic-sensor-tutorial/. [Accessed: 15-Sep-2021].
18. O'Grady, J. (2019). State of Charge Estimation of Lithium-ion Batteries using Extended Kalman Filtering. Retrieved from https://www.jackogrady.me/battery-management-system/state-of-charge-estimation-of-lithium-ion-batteries-using-extended-kalman-filtering/
19. Pandya, R. (2015). To Study and Use of Thermocouple for Temperature Measurement in Experiment Work.

Vol-1 Issue-4.

20. Process Parameters. (2019, June 24). What is a PT100 sensor working principle? Sensors UK manufactured. [Online]. Available: https://www.processparameters.co.uk/
21. Reese, L. (2019). The working principle, applications and limitations of ultrasonic sensors.
22. Veit, M., & Johra, H. (2021). How to use Arduino UNO for low-cost temperature measurements with Pt 100 sensors.
23. Yao, J., & You, F. (2020). Simulation-based optimization framework for economic operations of autonomous electric taxicab considering battery aging. Applied Energy, 279, 115721.
24. Zhang, X., Zhu, J., & Sahraei, E. (2017). Degradation of battery separators under charge–discharge cycles. RSC Advances, 7(88), 56099-56107.

Website References:

1. "Battery basics," Progressivedyn.com, (10-Nov-2020). [Online]. Available: https://www.progressivedyn.com/service/battery-basics/. [Accessed: 27-Feb-2021].

2. "Characteristics of lead-acid batteries," Pveducation.org. Available: https://www.pveducation.org/pvcdrom/lead acid-batteries [Accessed: 27 Feb-2021].

3. "Dip Trace - Schematic and PCB Design Software," Diptrace.com. [Online]. Available: https://diptrace.com/. [Accessed: 27-Feb-2021].

4. "ESP8266 daily task - publish temperature readings to ThingSpeak," Randomnerdtutorials.com, (2018). [Online]. Available: https://randomnerdtutorials.com/esp8266-daily-task-publish-temperature-readingsto-thingspeak/.

5. "Fee Schedule." PTA Pakistan Telecommunication Authority. (n.d.). Retrieved on September 9, 2021, from https://www.pta.gov.pk/en/industry-support/home/fee-schedule.

6. "Forbes Search," Forbes Magazine.

7. "How does a Pt100 sensor work?," Epicsensors.com. [Online]. Available: https://www.epicsensors.com/en/faq/how-does-a-pt100-sensor-work/. [Accessed: 15-Sep-2021].

8. "NodeMCU ESP32," Esphome.io. [Online]. Available: https://esphome.io/devices/nodemcu_esp32.html. [Accessed: 15-Sep-2021].

9. "The Internet of Things with ESP32," Esp32.net. [Online]. Available: http://esp32.net/. [Accessed: 15-Sep-2021].

10. "The role of cloud computing on the internet of things," Stonefly.com. [Online]. Available: https://stonefly.com/blog/role-cloud-computing-internet-things. [Accessed: 27-Feb-2021].

11. "What is Depth of Discharge, and why is it so important?" federalbatteries.com.au. (2020). Retrieved September 9, 2021, from https://federalbatteries.com.au/news/what-depth-discharge-and-why-it-so-important/

Saturn Publications

Frontiers in Engineering Science and Technology 1(2022) 2212–2221

www.saturnpublications/fest

Machine Learning Based Power Distribution System Reliability Improvement

Muhammad Usama Farooqi[1], Insharah Salman[2], Muhammad Mudassir Hussain[3], and Sardar Muhammad Maaz[4,*]

NED University of Engineering & Technology, Karachi, Pakistan

Received 12 March 2022; accepted 27 August 2022

Abstract

The task of maintaining optimum values of reliability by assessing parameters is becoming an ever-increasing challenge for utilities. This study focuses on optimizing values of SAIDI and SAIFI indices by implementing a Machine Learning (ML) based method known as Artificial Neural Network (ANN) on the IEEE 9 bus system. The system is modeled in the Simulink environment of MATLAB. The load busses of the system are then subjected to different faults that occur on the distribution network, which affects the reliability of distribution systems. The data collected by this process is used to train the ANN so it can detect and classify these faults. Since the focus of this study is on the distribution section, this means that only the three load busses are being considered for analysis. After the faults had been correctly detected and classified by the ANN, these results were then used to optimize SAIDI and SAIFI. In the next phase, software named Windmill was used for reliability analysis. The fault detection time calculated previously was used here to observe the updated conditions of the system and in the calculation of the improved values of SAIFI and SAIDI.

Keywords: Machine Learning (ML); Artificial Neural Network (ANN); MATLAB.

1. Introduction

The reliability of the Electrical Distribution System is vital for a country in different aspects. A reliable power system ensures an uninterrupted power supply to the consumers. Different parameters, such as the frequency of power outages, duration, and fault clearance time, can assess reliability. These parameters are directly linked to customer-oriented indices (SAIFI, SAIDI) and utility-oriented indices (ENS, AENS). In this project, the sole focus will be on customer-oriented reliability indices, including SAIFI and SAIDI.

SAIDI stands for System Average Interruption Duration Index (Yeddanapudi, 2016). It is the ratio of interruption duration to the number of customers served. In contrast, SAIFI stands for System Average Interruption Frequency Index (Power, 2022). SAIFI is the ratio of the total number of interruptions to the number of customers served.

The value of both of these indices computed for Karachi as per the 2019-20 NEPRA Performance Evaluation Report of Distribution Companies (Authority, 2019-20), comes out to be 27.56 for SAIFI % 2,655 minutes for value of both of these indices computed for Karachi as per 2019-20 NEPRA Performance Evaluation Report of Distribution Companies (AUTHORTY, 2019-20), comes out to be 27.56 for SAIFI and 2,655 minutes for SAIDI. Both these values exceed the standard values set by NEPRA, which are 16.22 for SAIFI and 649.48 minutes for SAIDI. This observation led to pondering the question of what can be done to make the distribution systems more reliable, and this serves as the motivation for this research.

In order to ensure the smooth execution of the proposed study, this project was divided into two phases. The SAIDI index was improved in the first phase, while the SAIFI index was optimized in the second phase. For the execution of the proposed study, IEEE 9 Bus System was first modeled on Simulink. The system was then subjected to different faults that affected the reliability, and data was collected for the training of ANN. After that, ANN was used to classify and detect these faults. For the implementation of ANN, the Levenberg-Marquardt algorithm was used. The timely detection and classification of faults by ANN will reduce restoring time, thus improving the Reliability of the Distribution Network. The detection time of different faults were noted down. Then these detection times were used to run reliability analysis on a software named Windmil, where it was observed that these detection times, after the integration of ANN, had led to significant improvement in SAIDI and SAIFI.

This study is an attempt to reduce the gap between threshold values and the existing values of the customer-oriented reliability indices. The complexity of distribution systems due to loads of variable nature at different time durations complicates the reliability of distribution

* Corresponding author

network. This study aims to solve the challenging problem of low-reliability indices and ensure that the system operates at the maximum possible reliability, ensuring a continuous supply of power to the consumers.

2. Objectives

In order to achieve the ultimate goal of optimum reliability, the project has been divided into the following objectives:

- To model IEEE 9 bus system based on SIMULINK MATLAB.
- To create the dataset for the training of ANN.
- To evaluate reliability indices (SAIFI, SAIDI) under normal and faulty conditions.
- To improve the index by using fault detection diagnosis and fault localization.
- To benchmark reliability indices with the base case.

After creating the data set for the training of ANN, ANN was trained for the detection and classification of different fault conditions, which include three-phase faults (ABC), line-to-line faults (AB, BC, CA), single line to ground faults (AG, BG, CG) and double line to ground faults (ABG, BCG, ACG).

3. Scope and Limitations

This project aims to provide a simulation-based algorithm that can be used to improve the reliability of a power system. The data required for this project has been gathered by running simulations on Simulink. So, this study is based on steady-state data acquired through simulation, and real time data is not used in this study. The system used for this study is according to IEEE standards. For evaluation of SAIFI and SAIDI, it has been decided to set equal load at all three load busses operating under normal loading conditions, and the load value considered is that of the bus which is loaded the most among the three as per IEEE standards. The decision to set the load equal at all three load busses is taken to simplify the algorithm's implementation. Furthermore, the main focus of this study is the distribution side of the power system, so the sole focus has been on load buses. Generation and transmission sections haven't been taken into account during analysis. Also, since the project's main concern is the reliability of distribution systems, only technical attributes of load buses like voltage and currents are considered, while protection and control aspects are out of the scope of this study. In addition to this, economic and environmental factors are also out of the scope as only technical analysis of the distribution system is considered.

4. Significance

Power supply interruptions have long plagued the power sector and caused significant challenges. Consumers suffer due to the unreliability of the electric power supply. In remote areas, where power interruptions are more frequent, consumers struggle to carry out their daily activities without access to electricity. The interruption of power can also result in substantial financial losses for industries, reducing output and damaging products. These are only a few of the issues encountered by consumers. From the utility's viewpoint, if the utility fails to meet the reliability indices specified by regulatory authorities, it may face regulatory penalties. Moreover, if the utility's reliability standards are insufficient, customers may leave their services and opt for a utility with better standards. This study seeks to address this major issue of poor reliability by optimizing the system, thereby benefiting both the consumer and the utility.

5. Literature Review

Power System

It has been observed that as the electrical power demand increases day by day, so does the system's vulnerability to faults. The increasing complexity of the power system's structure further complicates this problem. Therefore, traditional fault detection and classification methods cannot be relied upon as they rely on a reactive mindset rather than a proactive one, which results in greater fault clearance times and an overall increased number of fault occurrences. Moreover, 85-87% of faults occur in distribution lines (Baskar & Selvam, 2019; Singh, Panigrahi, & Maheshwari, 2011), and the consumer end of the power system is greatly affected. A possible solution to these problems can be found in using artificial intelligence and machine learning techniques for detecting and classifying faults (Baskar & Selvam, 2019).

According to (Baskar & Selvam, 2019; Youssef, 2009), some of the most widely used algorithms in this area include support vector machine (SVM), Bayesian Learner, Sequential Minimal Optimization (SMO), Logistic Regression, Decision Tree, and KNearest Neighbor. Upon further analysis, (Baskar & Selvam, 2019) found out that among these algorithms, the ones that yielded the most accurate results in power systems' fault detection and classification were those that implemented the supervised learning approach.

Reliability

Reliability refers to a measure of continuous accessibility of power to consumers. This can be evaluated in terms of the measurement and frequency of system breakdowns and their reestablishment time (Hartati, Sukerayasa, Setiawan, & Ariastina, 2007; Sucita, Mulyadi, & Timotius, 2018). The optimum reliability of a system ensures a sustained electric power supply to consumers. The evaluation of annual shutdowns, failures, and maintenance timeouts is obtained from the installed systems to calculate reliability indices such as SAIFI and SAIDI. The outcomes of these calculations aid in assessing

the existing state of the system's reliability as well as formulating necessary solutions to enhance reliability further (Sucita et al., 2018).

Reliability Enhancement

Due to unpredictability in loads and complexity in system structure, distribution systems suffer from approximately 90% reliability associated problems. This issue is to be mitigated to ensure uninterrupted supply. The approach used to rectify this issue involves implementing distributed generation (Ahmad, 2021; Short, 2018). Its impact was analyzed using modified particle swarm optimization for the placement of distributed generators (Ahmad, 2021; Gana, Aliyu, & Bakare, 2019). Analysis was performed for system reliability with and without distributed generation, and it was concluded that the SAIFI value decreased by 40% and SAIDI by 25% (Ahmad, 2021).

In (Hosseini, Shayanfar, & Fotuhi-Firuzabad, 2009), an algorithm for reliability testing is developed with the use of a Static Series Voltage Regulator (SSVR). SSVR can be employed efficiently to improve steady state voltage levels and reduce real and phantom power losses. According to (Hosseini, Shayanfar, & FotuhiFiruzabad, 2008; Hosseini et al., 2009), these can also be useful in reducing sags and under-voltage. The research involved testing a thirty-three and a sixty-six-bus standard distribution system. Both systems were evaluated for their reliability indices with and without the implementation of SSVR and then compared. To increase the efficiency of the performed test, it is evaluated with systems of two different proportions and placements. The results indicated an improvement in the system's reliability; however, the reliability was also affected by several other factors, including system capacity and placement as well as loading conditions.

Machine learning is developing rapidly over time and has been implemented in thousands of industrial and economic models. Likewise, it is expeditiously being utilized in power systems. In (Vaish, Dwivedi, Tewari, & Tripathi, 2021), the authors have established the importance of the use of ML-based techniques and methods in fault detection in power systems and how these methods provide an edge over conventional methods for fault detection and localization like impedance-based methods (Vaish et al., 2021; Verhelst, Van Ham, Saelens, & Helsen, 2017), traveling waves method (Vaish et al., 2021; Verhelst et al., 2017) and wide area fault localization (Mishra & Ray, 2018; Vaish et al., 2021) which are much more complex and time-consuming and due to the integration of DG's in existing grids, the complexity of these methods increases significantly.

Although ML-based methods are less complex and easy to implement, they also have downsides. For instance, the accuracy of detection and classification of faults depends upon the quality of the data set available. Since real data on power systems is not easily available, so simulation-based data is used for the implementation of ML-based methods. Neural Networks (Raza, Benrabah, Alquthami, & Akmal, 2020; Vaish et al., 2021) provide high accuracy when used for fault classification, but on the other hand, they require large amounts of data and memory for training. When using Support Vector Machines (Raza et al., 2020; Vaish et al., 2021), the chances of error in classification are quite low, but when used for multiclass classification, its complexity increases, and it requires a large amount of memory.

The K Nearest Method (MathWorks, 2016; Vaish et al., 2021) is easy to use and can be used as a base classifier; it takes a large amount of memory. All the discussion by (Vaish et al., 2021), leads to the conclusion that even though ML-based methods have certain lacking due to the unavailability of accurate power systems data available during their training, these methods can adapt more easily to the constant changes being made in modern grids due to integration of DG's as compared to conventional methods which would require extensive modifications with each change.

Deep learning is one example of a supervised learning approach in machine learning. Both (Mnyanghwalo, Kundaeli, Kalinga, & Hamisi, 2020) and (Jamil, Sharma, & Singh, 2015) have worked on this approach in the power sector. In (Mnyanghwalo et al., 2020), the authors have compared several deep learning approaches, including g Recurrent Neural Network (RNN), Long ShortTerm Memory LSTM), Gated Recurrent Unit (GRU), Feed Forward Neural Network (FFNN), and Artificial Neural Network (ANN). Among these, they found RNN to give the most accurate results. They also observed that the accuracy improved with the increase in network complexity, which is good for distribution systems since they are the most complex among all other electrical networks. In a study (Jamil, Sharma, Singh, 2015), the authors used Artificial Neural Networks to detect and classify faults

The neural net fitting tool of MATLAB has been used here to train the dataset using the Levenberg-Marquardt deep learning approach. The authors have trained a model for the detection and classification of single line-to-ground faults and have proposed that the same approach can also be used for all other types of faults.

After reviewing all of the discussions above, the authors concluded that machine learning has vast potential applications in improving the reliability of power systems. It was also observed that most of the contemporary research focuses either on fault detection and classification or on the improvement of reliability. The authors have therefore integrated the aforementioned two approaches so that the faults are detected and classified. At the same time, the impact of this is measured by measuring the reliability indices. The methods described in (Jamil et al.,

2015b) have been used as the basis for this study, and the techniques described in it have been used to train fault detection and classification models for all kinds of faults. This study has also used the Levenberg-Marquardt approach for this purpose.

SAIDI Improvement

According to (Balijepalli, Venkata, & Christie, 2004), within the continuously evolving world and with more reliance on uninterrupted electrical supply, improving the reliability of existing systems has become even more essential. For the provision of quality supply while regulating operation and maintenance budgets, every country's regulating authority specifies reliability standards and ranges to be maintained. Thus, the systems need to be operational at maximum efficiency to keep them within range. Moreover, constant research and up-gradation methods are required to be implemented to improve customer satisfaction while enhancing business for the utility. An important aspect of improving a power system's reliability is reducing the system's average interruption duration commonly termed (SAIDI).

SAIDI can be simply defined as the duration for which a customer encounters an electricity outage in a predefined time. The value for this index can be calculated daily, weekly, monthly, or yearly; however, a yearly calculation is conventionally used. A series of events can predominantly affect SAIDI values, including adverse weather conditions, mechanical failures, and repair times amongst others (Ajenikoko & Oladepo, 2018).

SAIFI Improvement

With the increase of competition in the modern energy market, with various utilities vying for control of the market, utilities tend to be conscious about the allocated budget being spent on operation and maintenance to provide the cheapest possible electricity to the consumers. The power regulatory authorities who are well aware of this scenario have started to keep an eye on the reliability of power being supplied by utilities so that the strict cost control being applied to the Operation and Maintenance budget does not come at the expense of consumers being suffered from poor reliability. So, certain reliability standards are to be met by utilities which are assessed on the basis of different reliability indices like SAIFI, for example. Utilities are being monitored by power regulatory authorities to ensure that they meet the specific value of reliability indices. If the example of SAIFI is considered, then in this power regulatory authorities want to make sure that the Operation and Maintenance budget is being spent on timely and proper maintenance so that customers suffer from as few outages as possible (Balijepalli et al., 2004; Holland & Cawley, 2006), (Balijepalli et al., 2004; Pennsylvania Public Utilities Commission %J M-00991220, 1999).

Various methods have been proposed to improve SAIFI. As Artificial Intelligence (AI) is being explored by researchers, many different AI-based methods are being put forward for the improvement of SAIFI. One such method is proposed in (Ahmad & Asar, 2021), in which Distributed Generations (DG) are being used, and by the application of AI, their optimum location of placement is determined as the farther the source is from the feeder less reliable the system is.

This study uses Artificial Neural Network (ANN), for this purpose and determines the optimal placement location of DG by considering different scenarios. The results show that by applying ANN, the authors were able to improve SAIFI by 40%.

6. Methods

To accomplish the study's objectives, the authors have used the MATLAB Simulink environment. The Simulink model of the IEEE-9 Bus System is taken from (Pettikkattil, 2022), and the methodology used for fault detection and classification has been adopted from (Jamil et al., 2015b), which has used binary logic to differentiate between different types of faults.

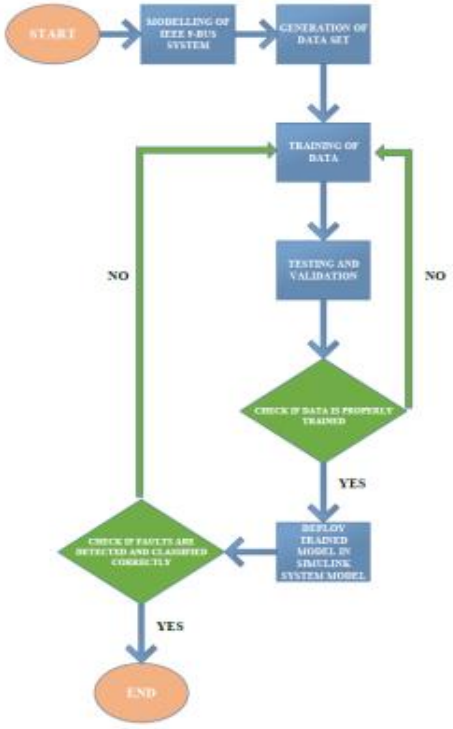

Fig. 1. Process Flow Chart

Modelling the Test System

An IEEE 9 bus system is modeled on SIMULINK to generate data for further analysis (Pettikkattil, 2022). It consists of three generation sources and three load buses. Focusing explicitly on the distribution buses, values of voltages, currents and sequence components are observed to identify fault cases.

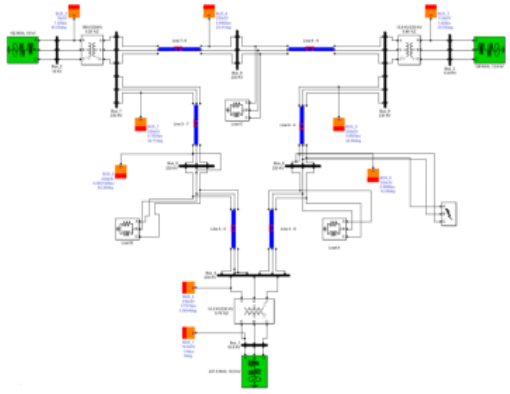

Fig. 2. Modelled Test System

Data Collection

The data is collected to perform two tasks as follows:

- Identify whether a fault has occurred or the system is un-faulted.
- Classify the type of fault that has occurred. To identify various fault cases, values of voltages, currents, and sequence components are recorded from simulations. Fault cases are identified based on the presence and absence of various sequence components. These values are stored in arrays and later used for training purposes.

Fault Type	Positive Sequence	Negative Sequence	Zero Sequence
Un-faulted	Present	Absent	Absent
Three phase faults	Present	Absent	Absent
Single line to ground fault	Present	Present	Present
Double line to ground fault	Present	Present	Present
Line to line fault	Present	Present	Absent

Fig. 3. Presence/Absence of sequence components of different faults

MATLAB codes are designed that use binary logic such as 0 for indication of un-faulted condition while 1 for faulted case, whereas, for fault classification, logic is designed such that the line on which fault occurs is 1, the remaining are labeled as 0 (Jamil et al., 2015b). The list of binary combinations generated is displayed below: A, B, and C represent lines, while G represents the ground—order of code bits: ABCG.

S.NO	Fault Type	Code
1	Un-faulted	0000
2	ABC	1110
3	AB	1100
4	BC	0110
5	AC	1010
6	ABG	1101
7	ACG	1011
8	BCG	0111
9	AG	1001
10	BG	0101
11	CG	0011

Fig. 4. Binary logic Codes used to describe different faults.

Data Training

The information collected is then processed by the deep learning algorithms to generate detection and classification filters for the system. Deep neural networks are used to design filters that are able to function in contemporary circumstances. They use a multi-network system to develop significant features that are required for intelligent detections in outputs (Anastasia Kyrykovych, 2022). For training the system values, MATLAB's NFTOOL is used. This tool is used to generate high-level relations and mapping between statistical input values and target data sets. It takes input and target data sets, trains them through a neural network algorithm, and provides a filter of required characteristics through either a MATLAB script or Simulink model (Ciaburro, 2022). The algorithm used for detection and classification in this project is the LEVENBERG-MARQUARDT algorithm. This algorithm involves the computation of additions of squared value of errors, establishing implementation on loss functions, gradient, and Jacobian matrices. This is an effective method to train datasets quickly and efficiently; however, for relatively large datasets, the system of processes becomes significantly complex and hence requires more memory compared to other algorithms. However, for the size of the data set considered in this project, this algorithm provided satisfactory results (Alberto Quesada, 2022).

Validation And Testing of Data

Detection

A total of 12000 samples are used, divided into three sets with 70% samples (8400) in training, 15% samples (1800) in validation, and 15% samples (1800) in testing. The training phase refers to adjustments of input parameters while training and setting output parameters. Validation and testing are performed to ensure proper training and efficiency of training (MathWorks, 1994-2022).

Results

	Samples	MSE	R
Training:	8400	2.07672e-9	9.99999e-1
Validation:	1800	2.08952e-9	9.99999e-1
Testing:	1800	1.92744e-9	9.99999e-1

Fig. 5. Performance of the trained detection model

The aforementioned results indicate overall efficiency and error in the training of data. MSE refers to "mean squared error is the average difference between outputs and targets, it is required to keep this value as low as possible." Whereas Regression R refers to the "measure of the correlation between output and target, here the value of R closer to 1 is required for accurate training" (MathWorks, 1994-2022). The results indicate successful training for fault detection. Next, a Simulink model can be generated to integrate into the main system.

Classification

Likewise for classification, a total of 12000 samples are used, divided into three sets with 70% samples (8400) in training, 15% samples (1800) in validation and 15% samples (1800) in testing.

Results

	Samples	MSE	R
Training:	8400	1.03146e-2	9.78582e-1
Validation:	1800	1.08096e-2	9.77449e-1
Testing:	1800	1.05216e-2	9.78019e-1

Fig. 6. Performance of the trained classification model

Observations

Once Simulink models are generated for both detection and classification, they are integrated with the main model. This model is simulated and tested for the detection and classification of different types of faults. An identical approach is implemented for the training of bus 5 and bus 8. Each bus has the following setup and configuration:

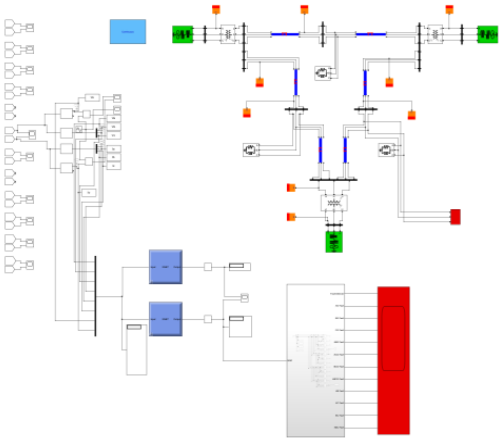

Fig. 7. Complete system setup for bus 6

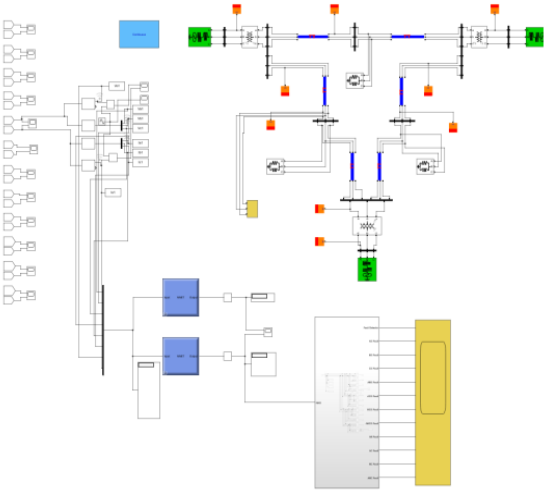

Fig. 8. Complete system setup for bus 5

The figures indicate data collection through workspace blocks, neural network blocks for detection and classification, bus voltages and currents through labels, and displays of various values through the scope. Through simulations, different faults can be induced in the system, which is successfully classified. For instance, when AG (line to ground fault is induced in the system's distribution buses), the detection block detects whether or not the system bus is faulted. Once this is determined, the type is configured. The following graphs indicate the presence and types of faults in the system. To summarize, to achieve the desired objectives of detection of classification of faults, the authors have first generated the required dataset by running simulations of the modeled IEEE 9-Bus System. Then MATLAB's Neural Fitting Tool was used for the training of this dataset, using the Levenberg-Marquardt algorithm of neural networks. Finally, a Simulink block has been generated after this training which is placed in the power system's model and is able to correctly identify and classify the different types of faults with speed and accuracy. Once fault detection and classification were implemented, the next task was to determine the fault detection duration. For this purpose, Simulink Profile Report was generated. This report displays the total simulation time, the time each block and process ran during each simulation cycle and other information.

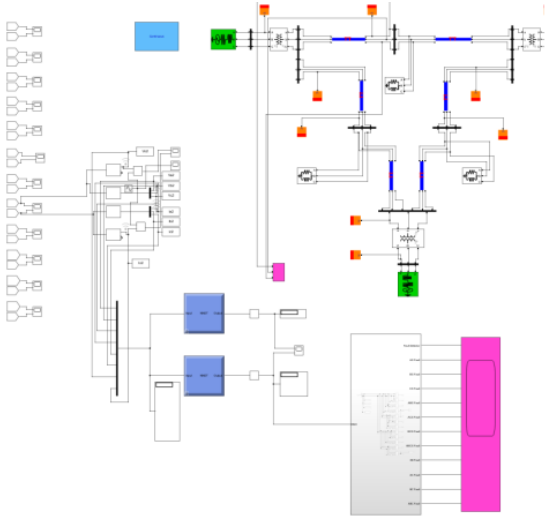

Fig. 9. Complete system setup for bus 8

Likewise, the detection time was calculated for all the fault cases and un-faulted conditions on each load bus. To analyze the system for the worst case, the highest detection time out of all three buses was selected for further calculations.

Reliability Analysis

To perform the reliability analysis, the authors used Windmil software, the idea for which came after reading (Bhusal, 2007). Windmil is software by Milsoft Utility Solutions that is used to run different simulated analyses on

power systems. The IEEE 9-bus system was modeled on this software, as shown in figure 9.

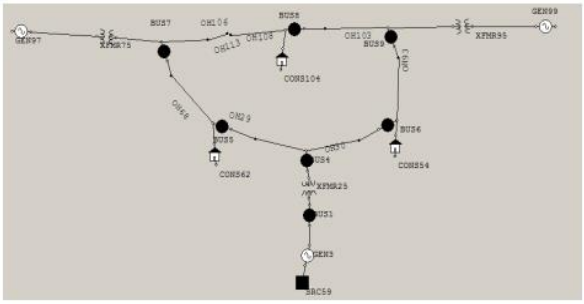

Fig. 10. Modelled System on Windmil Software

The time to detect and classify fault which came from MATLAB simulation was entered in the "Time to find problem" field of the Reliability Analysis Settings in Windmil, while all other settings were kept to their default values. Furthermore, the traveling time of the crew to the faulty location was selected as 30 minutes (DAZAHRA, 2021), as shown in figure 3.17, and it was considered that it would take equal time to reach any of the faulty busses for the sake of simplicity in analysis.

7. Results

This study was carried out using the MATLAB environment, while the reliability analysis was carried out on Milsoft Windmil software. The results from both of these softwares are discussed in this section.

Fault Detection and Classification

The phase and sequence values generated during a fault are captured and given as input to the trained Simulink model. Its results are sent to a binary logic classifier, which uses different logic gates to differentiate between different fault scenarios and displays the correct fault type that has occurred on the system. In the final output, the results are displayed on a scope, where a logic level of 0 determines which fault has not occurred on the system, and a logic level of 1 determines which fault has occurred on the system. One figure from each of the different fault scenarios (unfaulted, line-to-ground, double line-to-ground, triple line-to-ground, line-to-line) is shown below:

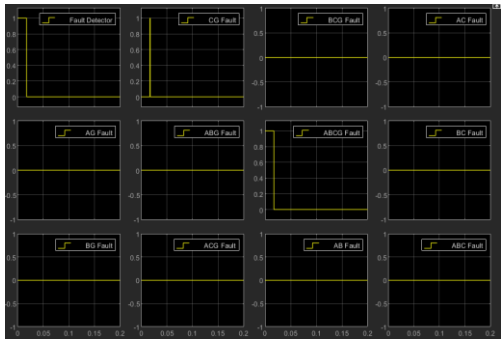

Fig. 11. Scope output showing no fault in the system.

Figure 11 indicates all faults are shown to be at a logic level of 0 that means no fault is induced on the system.

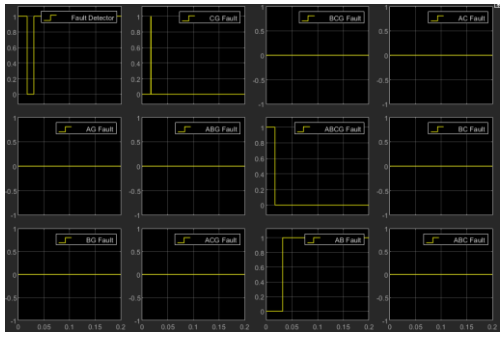

Fig. 12. Scope output showing Line-to-Line Fault between Phase A and B

Figure 12 shows that when a fault between Phase A and B is induced in the system the only the fault AB is shown to be at a logic level of 1, while the others are at a logic level of 0.

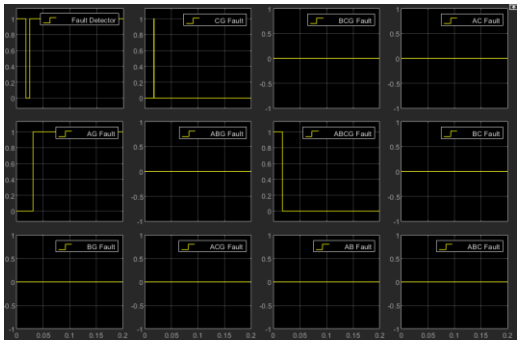

Fig. 13. Scope output showing Line-to-Ground Fault between Phase A and Ground

Figure 13 shows that when a fault between Phase A and ground is induced in the system only the fault AG is seen to be at a logic level of 1, while the others are at a logic level of 0.

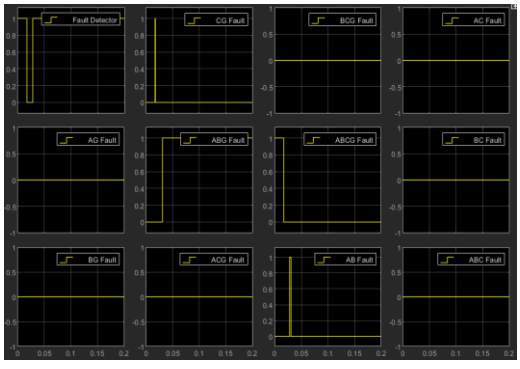

Fig. 14. Scope output showing Double Line-to-Ground Fault between Phase A, Phase B, and Ground

Figure 14 shows that when a fault between Phase A, B and ground is induced in the system only the fault ABG is seen to be at a logic level of 1, while the others are at a logic level of 0.

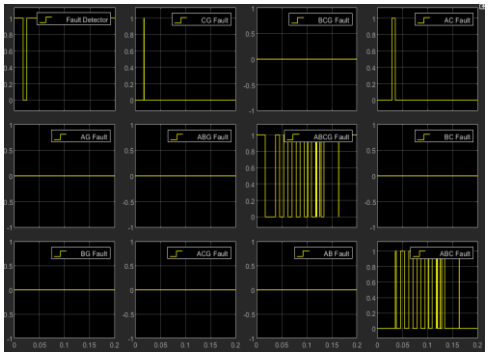

Fig. 15. Scope output showing Triple Line-to-Ground Fault between Phase A, Phase B. Phase C, and Ground

Figure 15 indicates that when a fault between Phase A, B, C, and ground is induced in the system, only the fault ABCG remains at a logic level of 1, while the others eventually reach the logic level of 0.

Similarly, for faults between Phase B and ground, the logic level of BG on the scope will be 1. For faults between Phase C and ground, the logic level of CG on the scope will be 1. For faults between Phase A, C and ground, the logic level of ACG on the scope will be 1. For faults between Phase B, C and ground, the logic level of BCG on the scope will be 1. For faults between Phase B and C, the logic level of BC on the scope will be 1. For faults between Phase A and C, the logic level of AC on the scope will be 1. For faults between Phase A, B and C, the logic level of ABC on the scope will be 1. In this way, all the types of faults are correctly classified by the trained model.

Reliability Analysis

According to (Abubakar & Aiyub, 2020), for an IEEE 9-bus test system, having the distribution section operating at 20kV, the values of SAIDI and SAIFI are calculated as 17.306 hour/customer.year and 1.130 faults/customer respectively. To enhance the reliability of the distribution system under observation, a machine learning algorithm termed Levenberg Marquardt algorithm was implemented. The values of SAIDI showed a decrease by 7.546% whereas SAIFI calculated after its implementation showed an improvement by 91.5%. The changes in the values of these parameters indicate a significant improvement in the overall reliability of the power system under inspection.

The main point to be noted here is that our modeled system was a small test system that was run mainly on theoretical conditions. That is why we see a significant improvement in the values of the desired indices. The improvement might not have been significant if it was a larger system with practical data. The main point to take away from this is that it is entirely possible to improve the reliability of a power distribution system by using Machine Learning algorithms, such as ANN, that have been used here, which was the whole purpose of this study.

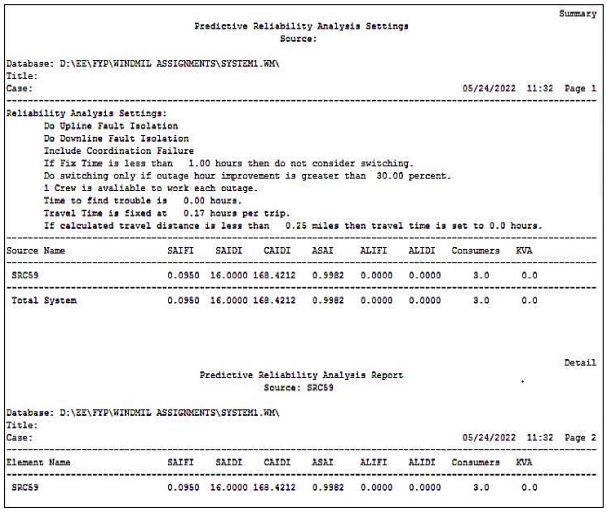

Summary

Predictive Reliability Analysis Settings
Source:

Database: D:\EE\FYP\WINDMIL ASSIGNMENTS\SYSTEM1.WM\
Title:
Case: 05/24/2022 11:32 Page 1

Reliability Analysis Settings:
Do Upline Fault Isolation
Do Downline Fault Isolation
Include Coordination Failure
If Fix Time is less than 1.00 hours then do not consider switching.
Do switching only if outage hour improvement is greater than 30.00 percent.
1 Crew is available to work each outage.
Time to find trouble is 0.00 hours.
Travel Time is fixed at 0.17 hours per trip.
If calculated travel distance is less than 0.25 miles then travel time is set to 0.0 hours.

Source Name	SAIFI	SAIDI	CAIDI	ASAI	ALIFI	ALIDI	Consumers	KVA
SRC59	0.0950	16.0000	168.4212	0.9982	0.0000	0.0000	3.0	0.0
Total System	0.0950	16.0000	168.4212	0.9982	0.0000	0.0000	3.0	0.0

Detail

Predictive Reliability Analysis Report
Source: SRC59

Database: D:\EE\FYP\WINDMIL ASSIGNMENTS\SYSTEM1.WM\
Title:
Case: 05/24/2022 11:32 Page 2

Element Name	SAIFI	SAIDI	CAIDI	ASAI	ALIFI	ALIDI	Consumers	KVA
SRC59	0.0950	16.0000	168.4212	0.9982	0.0000	0.0000	3.0	0.0

Fig. 16. Reliability Analysis Results

8. Conclusion

This study is a comprehensive take on the major issue of low reliability in current distribution systems. Ensuring optimum reliability in power supply systems is essential for both the utility and consumers. To track reliability, several indices have been formulated; however, in this study, the authors predominantly focused on SAFI and SAIDI, referring to the number of interruptions in the system and average interruption duration over a specified time duration. The main objective of this study was to model, simulate and analyze an IEEE 9 bus test system. Establish a dataset consisting of various parameters such as voltage, current, and sequence components. The generated dataset was then used to develop a fault detection and identification model. Levenberg-Marquardt algorithm was implemented for this purpose. Once a successful model was developed, it was used to determine fault detection time. This fault detection was used to calculate the values of SAIDI and SAIFI for the system under observation. The values were then compared to a benchmark system of similar specifications. A significant improvement in reliability indices was observed that was calculated after the implementation machine learning algorithm on the test system. A decrease of 7.546% in SAIDI and an improvement of 91.5% were observed in SAIFI. Hence by the implementation of Machine Learning, appreciable improvement in reliability was observed, thus, Machine Learning can provide exceptional assistance in improving the reliability of existing power systems.

9. Future Recommendation

The sole focus of this study has been on the distribution side of the system. In the future, this study can also be extended to transmission systems. In addition, real-time data of power systems can also be fed to the algorithm to give results in real-time, with the algorithm responding to real-time load fluctuations.

Besides this, by acquiring the maintenance and repair

history data of key components of distribution systems like Transformers, Circuit Breakers, and Cables from any utility company, a comprehensive study can be conducted about the predictive maintenance of these components by the integration of any ML-based method.

10. References

1. Abubakar, S., & Aiyub, S. (2020). *Reliability Analysis of 20 KV Electric Power Distribution System.* Paper presented at the IOP Conference Series: Materials Science and Engineering.

2. Ahmad, S. (2021). Reliability Enhancement of Electric Distribution Network Using Optimal Placement of Distributed Generation. *Sustainability, 13*(20), 11407.

3. Ahmad, S., & Asar, A. u. J. S. (2021). Reliability enhancement of electric distribution network using the optimal placement of distributed generation. *13*(20), 11407.

4. Ajenikoko, G. A., & Oladepo, R. A. J. I. (2018). Impact of System Average Interruption Duration Index Threshold on the Reliability Assessment of Electrical Power Distribution Systems. *6*(2), 17-31.

5. Alberto Quesada, A. (2022). 5 algorithms to train a neural network. Retrieved from: https://www.neuraldesigner.com/blog/5_algorithms_to_train_a_neural_network

6. Anastasia Kyrykovych, L. (2022). Deep Neural Networks. Retrieved from https://www.kdnuggets.com/2020/02/deep-neuralnetworks.

7. Authorty, N. E. P. R. (2019-20). *Performance Evaluation Report Distribution Companies* Retrieved from https://nepra.org.pk/Standards/2021/PER%20DISCOs%202019-20%20updated.pdf

8. Balijepalli, N., Venkata, S. S., & Christie, R. D. J. I. T. o. P. D. (2004). Modeling and analysis of distribution reliability indices. *19*(4), 1950-1955.

9. Baskar, D., & Selvam, P. (2019). Machine Learning Framework for Power System Fault Detection and Classification. *Int. J. Sci. Technol. Res, 9*.

10. Bhusal, P. (2007). *Distribution reliability analysis.* Wichita State University,

11. Ciaburro, G. (2022). How to use the Neural Fitting app (nftool). *MATLAB for Machine Learning* Retrieved from https://www.oreilly.com/library/view/matlab-formachine/9781788398435/636643bc-a7fb-4b8d-aba1-ec804d26363f.xhtml

12. Dazahra, M. N. (2021). Fault Location Isolation and Service Restoration. Retrieved from https://www.linkedin.com/pulse/fault-location-isolationservice-restoration-mohamed-nouh-dazahra/?trk=articles_directory

13. Gana, M., Aliyu, U., & Bakare, G. (2019). Evaluation of the reliability of distribution system with distributed generation using ETAP. *ABUAD Journal of Engineering Research and Development, 2*(1).

14. Hartati, R. S., Sukerayasa, I. W., Setiawan, I. N., & Ariastina, W. G. (2007). Penentuan Angka Keluar Peralatan Untuk Evaluasi Keandalan Sistem Distribusi Tenaga Listrik. *Universitas Udayana, Denpasar*.

15. Holland, W. F., & Cawley, C. J. H. (2006). *Electric service reliability in Pennsylvania 2005*.

16. Hosseini, M., Shayanfar, H. A., & Fotuhi-Firuzabad, M. (2008). Modeling of static series voltage regulator (SSVR) in distribution systems for voltage improvement and loss reduction. *Leonardo Electronic Journal of Practices and Technologies, 7*(12).

17. Hosseini, M., Shayanfar, H. A., & Fotuhi-Firuzabad, M. (2009). Reliability improvement of distribution systems using SSVR. *ISA transactions, 48*(1), 98-106.

18. Jamil, M., Sharma, S. K., & Singh, R. (2015a). Fault detection and classification in electrical power transmission system using artificial neural network. *SpringerPlus, 4*(1), 1-13.

19. Jamil, M., Sharma, S. K., & Singh, R. J. S. (2015b). Fault detection and classification in electrical power transmission system using artificial neural network. *4*(1), 1-13.

20. MathWorks. (1994-2022). Neural Net Fitting.

21. MathWorks. (2016). Introducing Machine Learning. Retrieved from https://www.mathworks.com/content/dam/mathworks/tagteam/Objects/i/88174_92991v00_machine_learning_section1_ebook.pdf

22. Mishra, D. P., & Ray, P. (2018). Fault detection, location and classification of a transmission line. *Neural Computing and Applications, 30*(5), 1377-1424.23.

23. Mnyanghwalo, D., Kundaeli, H., Kalinga, E., & Hamisi, N. (2020). Deep learning approaches for fault detection and classifications in the electrical secondary distribution network: Methods comparison and recurrent neural network accuracy comparison. *Cogent Engineering, 7*(1), 1857500.

24. Pennsylvania Public Utilities Commission %J M-00991220, D. (1999). Final Order on Reliability Benchmarks

and Standards, Docket no. *16*.

25. Pettikkattil, j. (2022). IEEE 9 Bus Retrieved from https://www.mathworks.com/matlabcentral/fileexchange/45936-ieee-9-bus

26. Power, K. (2022). System Average Interruption Frequency Index (SAIFI). Retrieved from https://kplc.co.ke/content/item/795/system-averageinterruption-frequency-index.

27. Raza, A., Benrabah, A., Alquthami, T., & Akmal, M. (2020). A review of fault diagnosing methods in power transmission systems. *Applied Sciences, 10*(4), 1312.

28. Short, T. A. (2018). *Distribution reliability and power quality*: Crc Press.

29. Singh, M., Panigrahi, B., & Maheshwari, R. (2011). *Transmission line fault detection and classification.* Paper presented at the 2011 International Conference on Emerging Trends in Electrical and Computer Technology.

30. Sucita, T., Mulyadi, Y., & Timotius, C. (2018). *Reliability evaluation of power distribution system with reliability Index assessment (RIA).* Paper presented at the IOP Conference Series: Materials Science and Engineering.

31. Vaish, R., Dwivedi, U., Tewari, S., & Tripathi, S. (2021). Machine learning applications in power system fault diagnosis: Research advancements and perspectives. *Engineering Applications of Artificial Intelligence, 106*, 104504.

32. Verhelst, J., Van Ham, G., Saelens, D., & Helsen, L. (2017). Model selection for continuous commissioning of HVAC-systems in office buildings: A review. *Renewable and Sustainable Energy Reviews, 76*, 673-686.

33. Yeddanapudi, S. R. K. (2 Sep 2006 - 16 Dec 2016). Distribution System Reliability Evaluation. Retrieved from https://web.archive.org/web/20111226034249/http://www.ee.iastate.edu/~jdm/ee653/DistributionReliabilityPredictive.ppt

34. Youssef, O. A. (2009). *An optimised fault classification technique based on Support-Vector-Machines.* Paper presented at the 2009 IEEE/PES Power Systems Conference and Exposition.

Saturn Publications

Frontiers in Engineering Science and Technology 1(2022) 2222-2228

www.saturnpublications/fest

Speed Control Optimization for Electric Vehicle Based on PI Controller

Abdul Rafay Bin Khalid[1,*], Izhaan Malik[2], Atiqa Gul Hassan[3], and Mohammad Abdur Rafay[4]

NED University of Engineering & Technology, Karachi, Pakistan

Received 12 July 2022; Accepted 30 September 2022

Abstract

With technological advancement and increased concern for controlling pollution, electric vehicles are becoming influential in the transport field. The Brushless Direct Current (BLDC) Motor is employed in electric vehicles converting electrical power into mechanical energy. Due to its low maintenance and compact structure, BLDC Motor technologies are widely used for global industrial applications, and variable speed drives in electric vehicles. This project aims to design the PI controller for speed control of BLDCM (Brushless DC Motor) used in electric vehicles and by using motor parameters monitored and controlled. The control parameters of the PI controller are Proportional Gain (KP) and Integral Gain (Ki), which are found in PI tuning. Simulation is carried out on different optimized algorithms showing the dynamic response for rapid tuning results of the proposed modified PI controller. The best-fitted optimized algorithm with smaller overshoot, less setting time, and rising time for the design of the controller is proposed, which can help control the motor's speed and maintain constant speed during load changes.

Keywords: Pollution Electric Vehicles; Brushless Direct Current (BLDC) Motor; PI Controller.

1. Introduction

Of the growing need for technological developments, sustainable energy utilization, and stringent rules and regulation for environmental safety, Electric Vehicles (EVs) are persistently acquiring significance in the automotive sectors (Khooban et al., 2017). EVs have a vast number of advantages, including smooth and quiet operation as well as high proficiency (Huang et al., 2009). Among the most used actuators in the construction of electric vehicles, Brushless DC Motos (BLDCM) are widely used (Has et al., 2017). The BLDCM includes various pretty properties, such as smooth speed control and better torque versus speed attributes, and is proposed for multiple applications due to its simple structure, high speed, minimal size, robustness, high efficiency, and reliable performance (Saravanan et al., 2020). Control of the DC motor's speed is generally done by adjusting the input voltage on DC motors. To control the speed of DC motors, various control techniques have been designed and applied in previous studies (Huang et al., 2009; Khatun et al., 2003].

From studies, the most widely used control technique for DC motors speed control is Proportional Integral Derivative (PID) technique due to its simplicity and effectiveness in control (Kalangadan et al., 2015). The execution of a regulator for speed control application is the main aim of this study. The conventional strategies are used to fix control parameters; Proportional Gain (Kp) and Integral Gain (Ki) found from PI tuning.

Numerous algorithms have been established to design the controller, especially swarms' behavior like GA (Ibrahim et al., 2019); BAT algorithm (Premkumar et al., 2015); cuckoo search algorithm (Murali et al., 2018), particle swarm optimization (Awadallah et al., 2009) flower pollination algorithm (Awadallah et al., 2009) and GOA (Potnuru et al., 2018) are used for BLDCM speed control. This work comprises of simulation of different algorithms showing the dynamic response for rapid tuning results of the proposed modified PI controller. Harris Hawks Optimization Algorithm (HHO) is the best fitted optimized algorithm with smaller overshoot, less settling time, and rising time for the design of the controller, which can help control the motor's speed and to maintain constant speed during load changes. HHO is a popular swarm-based, gradient-free optimization algorithm with several active and time-varying exploration and exploitation phases.

The main inspiration of HHO is the cooperative behavior, and chasing style of Harris' hawks in nature called surprise pounce. In this intelligent strategy, several hawks cooperatively pounce prey from different directions in an attempt to surprise it. Harris hawks can reveal a variety of chasing patterns based on the dynamic nature of scenarios and escaping patterns of the prey (Heidari et al., 2019). This work mathematically mimics such dynamic patterns and behaviors to develop an optimization algorithm. The

*Corresponding author

effectiveness of the proposed HHO optimizer is checked through a comparison with other nature-inspired techniques. The statistical results and comparisons show that the HHO algorithm provides very promising and occasionally competitive results. A basic flowchart about the operation of the complete system with the HHO algorithm is given in figure 1.

This study aims to design the PI controller for speed control of BLDCM used in an electric vehicle. The control parameters of PI are found from PI tuning. The system is modeled by state equations and transfer functions. Simulation for conventional PI and different Optimized algorithms are carried out, showing the dynamic response for rapid tuning results of the proposed modified PI controller. The best fitted optimized algorithm with smaller overshoot, less settling time, and rising time for the design of the controller is proposed to control the speed of BLDCM.

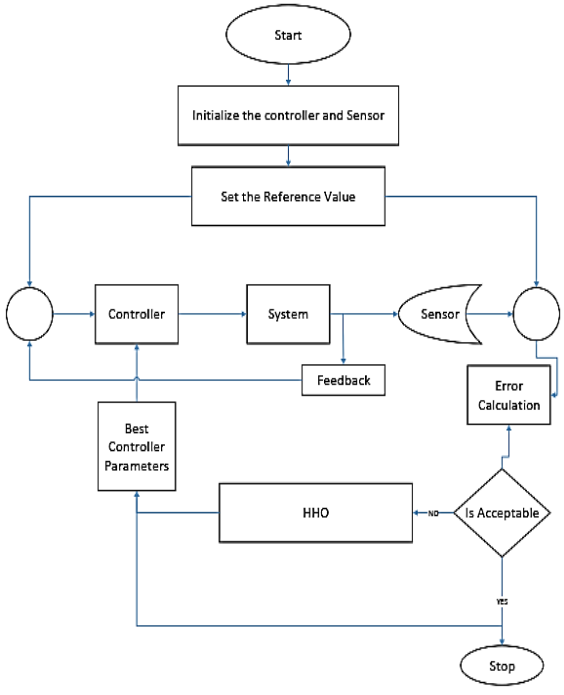

Fig. 1. Flow Chart of HHO

2. Objectives

The goal of this study is to meet the following objectives:

- To model the system with the interference of PI(Proportional Integral) controller.
- To optimize PI controller parameters for speed control of EV(Electric Vehicle) motor.
- To compare the proposed optimized result with the existing method.

3. Scope and Limitations

This design problem focuses on designing a controller to regulate the motor's speed rather than the motor's internal architecture. The system will be designed based on simulations, but due to time constraints, a prototype may not be produced to test the validity of simulation-based results and the controller's practicality. Even if a prototype is designed, then it might not be tested in EV due to its unavailability. Sensors will be inserted into the motor to measure its parameters; these sensors are based on electronics and have a thermal disadvantage.

4. Literature Review

In 2009, Huang et al. modeled the DC motor of an electric vehicle. A controller is designed with a differential geometric approach and linear quadratic regulator techniques to guarantee optimal performance. Ibrahim et al. (2019) produced an optimally designed controller of Brushless DC motor speed control depending on the genetic algorithm (GA). The result showed that the genetic algorithm designed PID has the finest relations to the rise time, settling time, and percentage overshoot than the conventional technique. Studies by Heidari et al. (2019) prove that HHO was capable of finding excellent solutions compared to other well-regarded optimizers.

Further, in 2020 Saravanan et al. designed a PI controller using a different algorithm and also debated with Grasshopper Optimization Algorithm (GOA) and Harris Hawks Optimization Algorithm (HHO). The motor parameters were monitored and controlled around the globe with the establishment of the Internet of Things (IoT). The results of the work show that the HHO controller yields the least error compared with other algorithms.

Author & Year	Objective	Result
Saravanan et al. 2020 [1902-1915]	Design PI controller using a different algorithm and also debated with Grasshopper Optimization Algorithm (GOA), Harris Hawks Optimization Algorithm (HHO). The motor parameters are monitored and controlled around the globe with the establishment of the Internet of Things (IoT).	• The BLDC motor model with the controller is developed in MATLAB. • Simulated results show HHO controller yields the least error.
Huang et al., (2009) [437-444]	An electric vehicle driven by a DC motor is modeled. A controller is designed with a differential geometric approach and linear quadratic regulator techniques to guarantee optimal performance.	• The performance of the designed controllers is compared with that of PID controllers. • The controller designed here demonstrates much better performance than that of the regular PID controller under test.
Ibrahim et al. (2019) [8694]	This article produces an optimally designed controller of Brushless DC motor speed control depending on the genetic algorithm (GA).	• The proposed controller has much better time response characteristics. • The genetic algorithm designed PID has the finest relations to the rise time, settling time, and percentage overshoot than the conventional technique
Premkumar & Manikandan, 2016 [818-840]	The design of fuzzy proportional derivative controller and fuzzy proportional derivative integral controller for speed control of brushless direct current drive has been presented using nature-inspired optimization algorithms such as particle swarm, cuckoo search, and bat algorithms.	• An optimized fuzzy proportional derivative controller has superior performance than the other controllers considered.

Heidari et al., 2019 [849-872]	In this paper, HHO technique is proposed to compete with other optimizers. For this purpose, a new mathematical model is developed in this paper.	• HHO was capable of finding excellent solutions compared to other well-regarded optimizers

Table 1. Reviewed literature summary: Optimization for Electric Vehicle based on PI Controller using different algorithms.

The review of literature hence validates the Optimization for Electric vehicles based on PI Controller using different algorithms. Results show that Brushless DC motors are one of the most used actuators in the construction of electric vehicles, with PID being one of the main used controllers. Different Techniques are employed for the designing of the controller of Brushless DC motors. Harris Hawks Optimization Algorithm gives the best-predicted outcome.

5. Methods, Observations and Calculations

The brushes in conventional DC motors wear out over time. Thus, the brushed DC motor cannot be used for operations that demand long life and reliability. To solve this problem, a brushless DC motor is used. The rotor of the BLDCM is a permanent magnet. The coil arrangement in the stator, when energized, will form an electromagnet. The operation of a BLDCM is based on the force interaction between the permanent magnet and the electromagnet.

A BLDC almost acts as a flipped version of a brushed motor because the permanent magnets become the rotor. Whereas the coil windings become the stator. There are motors with different magnet arrangements. Where the stator may have a different number of windings, and the rotor may have multiple pole pairs.

Dynamic Model

The phase voltages consist of voltage drop, resistance voltage drop, rate of flux linkages and the induced emf in the phase winding.

Van *= R.s ia + L.s dia/dt + ea* *(i)*

Vbn *= R.s ib + L.s dib/dt + be* *(ii)*

Vcn *= R.s ic + L.s dic/dt + ec* *(iii)*

Where ea, eb, ec are the induced EMFs in each phase. Van, Vbn, and Vcn are the phase voltages. R is the resistance per phase and L is the inductance per phase. These equations are represented in the matrix form:

$$\begin{bmatrix} van \\ vbn \\ vcn \end{bmatrix} = \begin{bmatrix} Rs & 0 & 0 \\ 0 & Rs & 0 \\ 0 & 0 & Rs \end{bmatrix} \begin{bmatrix} Ia \\ Ia \\ Ia \end{bmatrix} + \begin{bmatrix} dia/dt \\ dib/dt \\ dic/dt \end{bmatrix} + \begin{bmatrix} e & a \\ e & b \\ e & c \end{bmatrix}$$

Transfer Function

The transfer function is the ratio of the Laplace Transform of output to the Laplace Transform of input when all the initial conditions are assumed to be zero. The transfer function of a system has an important part in determining the response of a system. Consider the load torque on the system equal to zero. If a certain armature voltage is supplied, a speed (ws) is attained.

Figure 2. shows the block diagram between voltage and speed. Block diagram reduction techniques are used to develop the transfer function for the BLDCM (Xia, 2012).

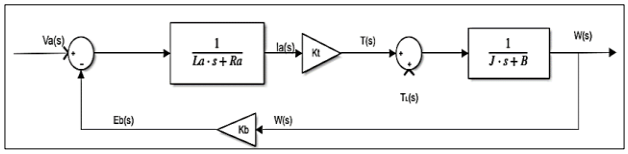

Fig. 2. Transfer Function of the BLDC Motor

$$\frac{\omega(S)}{v(S)} = \frac{k}{(La \cdot S + R_a) + (J_S + B) + K_2}$$

Back EMF

Motors act as a generator when they are rotating. This means that a back-EMF voltage is induced in the stators, which opposes the driving voltage of the motor. Back EMF is an important characteristic of a motor as by looking at its shape; it can be determined what type of motor is in use. And it also indicates the type of control algorithm that is needed to be used to control the motor. BLDCs have a trapezoidal shape and are commonly controlled by trapezoidal control (Pimentel et al., 2013). An easy way to observe the back-EMF shape is to use simulation. A one-pole pair BLDC motor is simulated with open-circuit terminals.

Inner Configuration of BLDC

There are six possible ways of energizing coil pairs. By commutating two phases at a time, the stator magnetic field is made to rotate, which will cause the rotor to turn. The rotor angle is measured concerning the horizontal axis with six different rotor alignments. If the correct phases every 60 degrees are commutated, it will make the motor spin. This is called six-step commutation or trapezoidal control (Xia, 2012). It is observed that with more pairs of poles, the commutation occurs more frequently. To properly commutate the motor at the right times with the correct phases, the rotor position is needed to be known. Which is usually measured by using hall sensors. The poles of the same kind repel each other, making the rotor turn counterclockwise. At the same time, the opposite poles attract each other, and the rotor keeps on turning in the same direction. Once it completes 60 degrees (for single pole pair) of rotation, the next commutation occurs. The commutation occurs in such a way that the rotor never aligns with the stator magnetic field, but it is always chasing it. Two things can explain this behavior.

1. When the rotor and stator magnetic fields align perfectly, the motor creates zero torque. It is not to be aligned.
2. Maximum torque occurs when the fields are at 90 degrees to each other. The desired outcome is to bring this angle close to 90 degrees. In BLDC motor, 90 degrees can never be achieved with six-step commutation. But the angle fluctuates within some

range. This is due to the simple nature of trapezoidal control.

Six-Step Commutation Logic (HALL Sensor)

The selected Brushless DC motor has three coil windings in the stator and a single pole pair in the rotor. Two phases are energized simultaneously: positive DC (north pole) and negative DC (south pole). This occurrence leads to simultaneous attraction and repulsion between the stator and rotor. In the simulation, the hall effect sensor wmodeledled based on relational operator and AND gates to select the sector based on the relations. In order to choose a switching pattern logic based on sector, a multiport switch has been used in the simulation. The selected sector number is used as the first input to the multiport switch to tell which sector's logic pattern is required for proper commutation for continuous rotor rotation.

Pulse Width Modulation

The desired outcome is to make the motor spin at different speeds. A constant DC voltage is used at the input to the inverter, which leads to constant speed. The voltage can be adjusted by closing the loop with a suitable controller; based on the difference between the desired and measured speed, the controller will adjust the voltage to bring the motor speed close to the desired value. An ideal voltage source is used to generate different DC voltage levels commanded by the controller. But in reality, the DC voltage supplies a fixed voltage which is needed to be modulated using a technique called PWM before providing it to the three-phase inverter. PWM is a square wave signal that repeats itself at a certain frequency. The longer the duty cycle the higher the voltage. PWM control has an averaging effect on the output voltage that is sensed by the motor. Frequency of PWM must be selected very carefully. If the frequency is too low, instead of observing an averaged voltage the model will observe a voltage that tries to follow the square wave shape, this will lead to poor tracking of the reference speed and the motor will keep speeding up and slowing down. However, if the frequency is increased to certain reasonable value the voltage will be averaged out, which will improve the speed control performance. The ripples will occur due to the switching nature of PWM. The frequencies normally are on the order of a few kilohertz and need to be selected to be much higher than the reciprocal of the motor time constant.

Practical Motor Selection

The Brushless DC motor has multiple applications, however, the main focus in this system is BLDCM used in electric vehicle. The Brushless DC motor is mainly used in small EVs like e-bikes and e-cycle. It was observed while researching that 250W BLDC motors are being used frequently to power e-bikes ("Top 20 Cheapest Electric Scooters, n.d.) therefore, a 250W BLDC motor manufactured by Maxon company (maxon EC 45) was selected for this system. The parameters of the system were taken from ("EC 45 Ø45 mm, March 2021).

Nominal speed (rpm)	4300
Nominal torque (mN.m)	331
Max. efficiency	85 %
Phase-Phase resistance	0.43 Ohm
Ph-ph inductance	0.17 Mh
Torque constant (mNm/A)	45.5
Speed constant (rpm/V)	210
Rotor inertia gcm2	209
Damping Factor (Nm/rad/s)	0.000735

Table 2. Motor Parameters

Proportional Integral Controller

For speed control, a discrete PI controller is used. The PI controller is responsible for generating the necessary voltage that will cause the motor to run at the desired speed; if the tuning parameters are selected correctly, then the motor will be able to respond quickly with minimum overshoot and high stability. There are multiple methods to tune PI parameters (kp and ki) for optimal rise time and overshoot. Model based tuning method in MATLAB was used to determine the constants for the controller. Manual methods like pole placement and loop shaping in which the position of poles and zeros of the PI-controller in an s-plane can be used to vary response and gains. However, this method was found to be less accurate; therefore automatic MATLAB based tuning method was used for determining controller constants, in which gains are automatically calculated with respect to the selected system's response characteristics. After inserting the tuned constants in the PI block, the system's response to varying loads was fast and accurate.

Model-based tuning can also be done on the model's transfer function estimated through MATLAB's system identification toolbox or linear analysis tool. However, the complex control of the BLDC motor resulted in inaccurate transfer functions. As a result, automatic tuning was directly used on Simscape blocks of the system for accurate observations.

Transfer Function based auto tuning	**Kp**	**Ki**
0.05	**0.0**	

Table 2. Controller Values

On the above grounds, we conclude that the transfer function of a system has an important part in determining the response of a system. Motors act as a generator when they are rotating. This means that a back-EMF voltage is induced in the stators, which opposes the driving voltage of the motor. BLDC motors has a Trapezoidal back EMF. There are six possible ways of energizing coil pairs. The stator magnetic field is made to rotate by commutating two phases at a time. Which will cause the rotor to turn The desired outcome is to make the motor spin at different speeds. A constant DC voltage is used at the input to the inverter, leading to constant speed. The buck converter is used to adjust the DC source voltage to different voltage levels in order to be able to control the BLDCM at varying speeds discrete PI controller is used. The PI controller is responsible for generating the necessary voltage that will cause the motor to run at the desired speed. The system must have a greater response time and less peak time,

overshoot, and settling time. The behavior of a transfer function in the transient response is determined by calculating the rise time, peak time, settling time, and overshoot (Fadali & Visioli, 2012; Bolton, 2021). These values determine if the system is overdamped, underdamped, critically damped, or undamped.

Harris Hawks Algorithm

A novel population based meta heuristic algorithm with new nature inspired technique. The main idea behind HHO is inspired by the cooperative behaviors of one of the most intelligent birds called Harris hawks and its behavior of hunting prey. Meta-heuristic algorithms have been designed and utilized for tackling many problems as competitive alternative solvers because of their simplicity. The main inspiration of the HHO algorithm is the Harris hawks team's behaviors of hunting and chasing patterns for the capture of prey in nature. This algorithm has been implemented to determine the optimal values of PI tuned parameters kp and, ki. The different phases of the HHO algorithm can be seen in figure 3 below (Heidari et al., 2019).

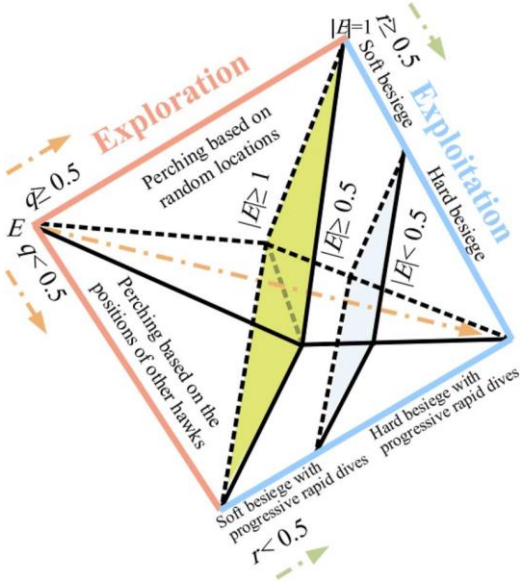

Fig. 3. Phases of Harris Hawks Algorithm

6. Results

The system was modeled in two ways to observe the effects of speed control optimization in a Brushless DC motor.

- Manual control
- Auto-control with PI controller

The obtained results are discussed below. Furthermore, a comparative analysis has been done between the results of both systems.

Manual Control

In this system, Brushless DC motor, 3-phase inverter, and its rotational logic were modeled without PI controller and PWM generator. The only way to control the motor's speed is by manually controlling the DC voltage supply.

The higher the DC voltage supply greater will be the motor's speed as observed in fig. 4. When the DC supply was 24V, the measured speed of motor was around 210 RPM. Similarly, when supply was 50V, the measured speed was around 430 RPM. This method is not practical since manual control would require 24/7 monitoring of the motor's desired speed. The modeled system is shown in fig 4. This drawback necessitates the use of a PI controller for automated speed controlling of the BLDC motor.

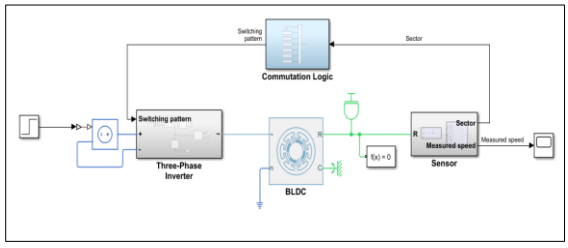

Fig. 4. BLDC Simulation on Matlab without PID

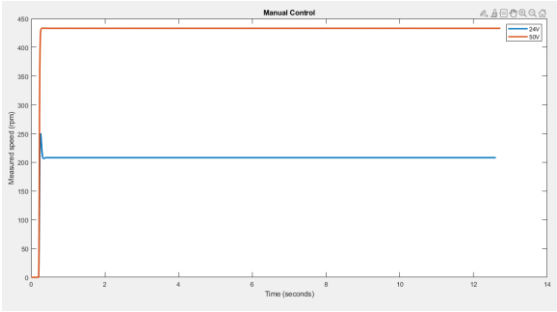

Fig. 5. Manual Control BLDC Simulation

Automatic Control With PI

PI controller was incorporated to measure the error between demanded and measured speed. This steady state error is then eliminated by supplying the required voltage (duty cycle) to the PWM generator. This model was simulated on MATLAB; motor parameters were taken according to the selected motor's data sheet. Varying demanded speed was given as input to the comparator, which compares the value of the required speed with the measured speed coming from a closed feedback loop, as seen in figure 6.

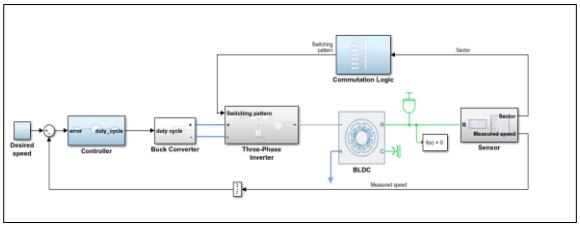

Fig. 6. BLDC Simulation on Matlab with PI Controller

Simulink's repeated sequence block was used to create a varying demanded speed scenario. It was set to be varied every 5 seconds to observe controller's response through measured speed. It was observed that the system's response time was rapid to demanded speed variations as shown in figure 7.

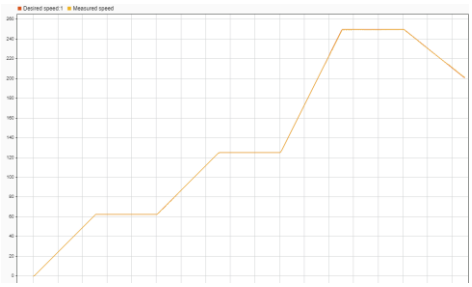

Fig. 7. Automatic Control BLDC Simulation

7. Conclusion and Future Implications

Simulink was used to successfully model and simulate the system presented in the initial proposal. A 250W BLDC motor was selected whose trapezoidal back EMF was used to sense the rotor position. Commutation logic was created using designated sectors of rotors monitored with a Hall sensor. This commutation logic was used in a 3-phase MOSFET-based inverter circuit that converted DC-AC voltage and energized two output phases at the same time to ensure proper motor rotation. The system's response was overdamped, which can only be controlled by varying supply voltage manually in case of varying loads.

Therefore, PI controller was developed for the motor's speed control. An automatic model based tuning method was applied to the PI controller to determine the controller constants. A Pulse Width Modulation (PWM) generator was used to generate different voltages for different demanded speeds through duty cycle variation to control the DC voltage supplied to the inverter. This duty cycle variation is done through PI controller, which converts the error difference into the required duty cycle to eliminate the steady state error. This modeled system was simulated successfully, resulting in a rapid system response to variable speed demands.

8. Practical Implementation

This project should be practically implemented in the future in order to verify the computed results in real time. Moreover, this project was completely based on MATLAB simulations which indicate that the results might be different if a prototype is designed in a practical world where the computed parameters will be subjected to multiple intermittent practical constraints.

Optimized Algorithm

Multiple algorithms like probabilistic, heuristic, and meta-heuristic algorithms have already been developed. Harris Hawks algorithm was just one implementation to find the tuned parameters in this project. There are multiple other algorithms that can be tested on this system in the future, like particle swarm optimization, Ant Lion Optimization algorithm, gradient descent algorithm, leader Harris Hawk's algorithm, etc. might be able to produce more optimized results than the HHO.

Fractional Order PI Controller

A fractional version of the PI controller called as FOPI controller has been designed as an advancement of PI controller. A comparative analysis of PI and FOPI controllers can be made by checking its performance on controlling a BLDC motor.

Learning can provide exceptional assistance in improving the reliability of existing power systems.

9. References

1. Awadallah, M. A., Bayoumi, E. H., & Soliman, H. M. (2009). Adaptive deadbeat controllers for brushless DC drives using PSO and ANFIS techniques. *Journal of Electrical Engineering*, *60*(1), 3-11.
2. Bolton, W. (2021). Chapter 2-Instrumentation system elements. *Instrumentation and Control Systems, 3rd ed.; Bolton, W., Ed*, 17-70.
3. EC 45 Ø45 mm, brushless, 250 Watt, with Hall sensors" March 2021. Accessed on: Feb. 26, 2022. [Online].
4. Fadali, M. S., & Visioli, A. (2012). *Digital control engineering: analysis and design*. Academic Press.
5. Has, Z., Muslim, A. H., & Mardiyah, N. A. (2017, September). Adaptive-fuzzy-PID controller based disturbance observer for DC motor speed control. In *2017 4th International Conference on Electrical Engineering, Computer Science and Informatics (EECSI)* (pp. 1-6). IEEE.
6. Heidari, A. A., Mirjalili, S., Faris, H., Aljarah, I., Mafarja, M., & Chen, H. (2019). Harris hawk's optimization: Algorithm and applications. *Future generation computer systems*, *97*, 849-872.
7. Huang, Q., Huang, Z., & Zhou, H. (2009). Nonlinear optimal and robust speed control for a light-weighted all-electric vehicle. *IET Control theory & applications*, *3*(4), 437-444.
8. Ibrahim, M. A., Mahmood, A. K., & Sultan, N. S. (2019). Optimal PID controller of a brushless DC motor using genetic algorithm. *Int J Pow Elec & Dri Syst ISSN*, *2088*(8694), 8694.
9. Kalangadan, A., Priya, N., & Kumar, T. S. (2015, November). PI, PID controller design for interval systems using frequency response model matching technique. In *2015 International Conference on Control Communication & Computing India (ICCC)* (pp. 119-124). IEEE.
10. Khatun, P., Bingham, C. M., Schofield, N., & Mellor, P. H. (2003). Application of fuzzy control algorithms for electric vehicle antilock braking/traction control systems. IEEE Transactions on Vehicular Technology, 52(5), 1356-1364.
11. Khooban, M. H., ShaSadeghi, M., Niknam, T., & Blaabjerg, F. (2017). Analysis, control, and design of speed control of electric vehicles delayed model: multi-objective fuzzy fractional-order controller. *IET Science, Measurement & Technology*, *11*(3), 249-261.
12. Murali, S. B., & Rao, P. M. (2018, January). Adaptive sliding mode control of BLDC motor using cuckoo search algorithm. In *2018 2nd International Conference on Inventive Systems and Control*

(ICISC) (pp. 989-993). IEEE.

13. Pimentel, J. C., Gad, E., & Roy, S. (2013, December). Stability analysis of BLDC motor speed controllers under the presence of time delays in the control loop. In *2013 International Conference conducted on Connected Vehicles and Expo (ICCVE)* (pp. 171-176). IEEE.
14. Potnuru, D., & Tummala, A. S. (2018, August). Implementation of grasshopper optimization algorithm for controlling a BLDC motor drive. In *Soft Computing in Data Analytics: Proceedings of International Conference on SCDA 2018* (pp. 369-376). Singapore: Springer Singapore.
15. Premkumar, K., & Manikandan, B. V. (2016). Bat algorithm optimized fuzzy PD based speed controller for brushless direct current motor. *Engineering Science and Technology, an International Journal*, *19*(2), 818-840.
16. Saravanan, G., Ibrahim, A. M., Kumar, D. S., Vanitha, U., & Chandrika, V. S. (2020). Iot based speed control of bldc motor with Harris hawks optimization controller. *International Journal of Grid and Distributed Computing*, *13*(1), 1902-1915.
17. "Top 20 Cheapest Electric Scooters available in India," Jan. 11, 2022. Accessed on: Feb. 25, 2022. [Online].
18. Xia, C. L. (2012). *Permanent magnet brushless DC motor drives and controls*. John Wiley & Sons.

Saturn Publications

Frontiers in Engineering Science and Technology 1(2022) 2229-2234

www.saturnpublications/fest

Is Thermal Power Plant a Better Alternative to Coal Fired Power Plant? A Comparative Analysis

Muhammad Hassan Khan[1,*], Manahil Fatima[2], Sohail Ahmed[3], and Shaheryar Ali[4]

Dawood University of Engineering & Technology, Karachi, Pakistan

Received 10 June 2022; Accepted 16 September 2022

Abstract

Thermal power plants are used worldwide to generate electricity by using heat energy. The thermal power plants in Pakistan are outdated and inefficient and use expensive fuel to generate electricity which has a huge environmental impact. Thermal power plants not only lead to air pollution but also have serious impacts on land and soil. The existing thermal power plant's efficiency can be improved by using imported coal which will reduce emissions and reach the increasing demand for electricity in the country. The government of Pakistan is currently interested in installing a coal-fired power plant. A coal-fired plant is a power plant in which electricity is generated by burning coal as steam is produced. The need to install a coal-fired power plant in Pakistan arises due to the lack of technology to process the coal that the country receives from the coal reserves in Thar. The amount of coal in Thar is huge, but its quality is considered low, and it needs significant investment in infrastructure for extraction and processing. The coal-fired power plant provides affordable and reliable constant power that can meet the country's demand for energy consumption. But it also has a negative impact on our environment. However, both plants have a considerable impact on the environment. Thermal power plants usually emit large amounts of mercury and fly ash which, one way or another, destroys our environment. These power plants discharge large volumes of wastewater, containing vast quantities of pollutants, into the waters, and these discharge pollutants cause severe health and environmental problems. As coal is burned in the coal-fired plant, a number of pollutants are released. Air pollution from coal-fired power plants can cause asthma, cancer, neurological problems, and global warming. A major man-made contributor to climate and global warming is the release of greenhouse gases into the atmosphere from power plants. However, measures have been put in place to reduce the environmental impact, such as regular ecological monitoring should be done to ensure compliance with the relevant regulations and standards. Overall, the government of Pakistan and the public need to work together and present effective ideas to develop and implement the required solutions that will increase economic growth and should take steps to minimize the environmental impacts caused by the power plants. And efforts should be made to improve the efficiency of both plants cost-effectively.

Keywords: Thermodynamics; Thermal Power Plants; Coal-Fired Plants.

1. Introduction

Thermal power plants can be described as power stations in which heat energy is converted into electrical energy. The thermal power plant uses various fuel sources like natural gas, coal, oil, and nuclear power to generate electricity. In a Thermal power plant, heat is produced by burning different fuel sources (natural gas, coal), which generate electricity. Steam is produced by the heat (produced by the burning of fuels), which then drives a turbine to generate electricity. The produced steam is then condensed and recycled back into the system. Thermal power plants were initially established as a backup to hydropower. Transmission losses have become an important issue over long distances. Thus, thermal power was intended to facilitate the areas difficult to be served by hydropower. The rational thermal power base has been developed and is controlled by three major players, i.e., WAPDA, Independent Power Producers (IPPs), and Karachi Electric (KE).

The first coal-fired plant in the 19th century used reciprocating engines to generate direct currents. These plants generate electricity by burning coal in a boiler to produce steam, which then flows into a turbine to spin a generator. Coal-fired power stations are a major contributor to climate change, emitting 10 Gt of carbon dioxide and about one-fifth of the world's greenhouse gas. There are four main types of coal-fired power stations: subcritical, supercritical, ultra-supercritical, and cogeneration, which vary in efficiency.

The usage of different fuels leads to the difference between both the power plants. A thermal power plant uses a variety of fuels, such as natural gas, coal, and even biomass, to produce steam to generate electricity. Whereas

*Corresponding author

coal-fired power plants rely solely on coal as a fuel to generate electricity.

The overall efficiency of the power sector of Pakistan is 0.907. The efficiency of the thermal power plant is defined as the ratio of heat equivalent of output electrical energy to the heat of coal combustion. The overall efficiency of a modern thermal power plant is about 29%. In contrast, coal-fired plants are less efficient than other thermal power plants as they have lower heat-to-electricity conversion rates. This plant also produces more greenhouse gas emissions and air pollutants. Coal-fired power plants hold the upper hand in producing electricity on demand, making them more reliable. They are considered more reliable and affordable than other thermal power plants, at least in countries like Pakistan with large coal reserves. Both plants have a negative impact on the environment and cause severe health problems. The government should make efforts to reduce these impacts.

In conclusion, both power plants are used worldwide to generate electricity. The thermal power plant is more efficient and environmentally friendly than coal-fired power plants as coal-fired plants produce more air pollutants. But coal-fired plants are more affordable and reliable.

2. Literature Review

Shutting Down of Thermal Power Stations

In recent years, several thermal power stations in Pakistan have been shut down, leaving the country with a severe electricity crisis. Pakistan is currently facing a severe foreign exchange crisis, which is leading to a shortage of foreign currency that is needed to import fuel and equipment for the operation and maintenance of its thermal power stations. This shortage of foreign exchange has also resulted in making it difficult to invest in the construction of new power plants with modern technology, which will be much more efficient and will also result in generating more electricity.

Block	Description	Reference Fuel Cost Component (Rs./kWh)	Revised Fuel Cost Component (Rs./kWh) w.e.f 15-10-2019
		Furnace Oil	Furnace Oil
I	Jamshoro Unit 1	19.5519	21.4749
II	Jamshoro Unit 2	21.9576	24.1173
II	Jamshoro Unit 3	21.3659	23.4674
II	Jamshoro Unit 4	20.916	22.9732

Fig. 1. Fuel cost revision for the FY 2019 of Jamshoro Power Plant.

Technical Reasons with Justifications for Shut Down:

i. Unavailability/High Prices of Fuel:

The main reason for the shutdown of thermal power stations in Pakistan is the result of the unavailability of furnace oil, which is the fuel required to generate electricity. With minimal refining capacity, Pakistan relies heavily on imported fuel to meet the demand. As the country is facing extreme foreign exchange crises, it becomes expensive to import fuel, leading to a fuel shortage.

Moreover, the domestic production of furnace oil has also declined over the years, leading to an increasing reliance on imported fuel. The lack of fuel has reduced electricity generation from thermal power plants, contributing to frequent power outages and load shedding.

According to the Pakistan Bureau of Statistics, the country's oil production declined from 24.8 million barrels in 2012-13 to 19.5 million in 2019-20. This decline in domestic production has resulted in an increasing reliance on imported fuel. In the fiscal year 2020-21, Pakistan imported 11.4 million metric tons of petroleum products worth $4.4 billion, up from 10.4 million metric tons worth $3.8 billion in the previous year.

Period	Description	Reference FCC Rs./kWh	Revised FCC Rs./kWh
August 2022	Block I Unit 1	19.5519	43.8050
	Block II Unit 2	21.9576	49.1948
	Block II Unit 3	21.3659	47.8691
	Block II Unit 4	20.9160	46.8612

Fig. 2. Fuel cost revision for the FY 2022 of Jamshoro Power Plant.

ii. Outdated Technology:

Another major justification for the shutdown of thermal power stations in Pakistan is the use of outdated technology. Many of the thermal power plants in Pakistan were constructed several decades ago and are still using technology that is no longer efficient or cost-effective. The outdated technology leads to higher electricity production costs and contributes to environmental pollution.

The use of outdated technology in thermal power plants also makes it difficult to maintain and repair the power plants, leading to frequent breakdowns and shutdowns. As a result, the electricity produced by these plants is often unreliable, leading to frequent power outages and load shedding. According to the Pakistan Energy Yearbook 2019-20, the thermal power generation in Pakistan was around 24,325 GWh, with a total installed capacity of 22,931 MW. Out of this, the share of oil-fired thermal power generation was about 16,317 GWh, with a total installed capacity of 8,257 MW. Many of these oil-fired thermal power plants in Pakistan use outdated technology, some of which are over 30 years old. For instance, the Jamshoro Thermal Power Station in Sindh province was commissioned in 1989 and still uses technology from that era.

Furthermore, the National Electric Power Regulatory Authority (NEPRA) has identified several issues with the operation and maintenance of thermal power plants in Pakistan due to outdated technology. In its annual report for the fiscal year 2019-20, NEPRA reported that the efficiency of thermal power plants run on fuel in

Pakistan was only around 36%, compared to the global average of 46%.

iii. Environmental Concerns:

Thermal power plants in Pakistan are a significant source of environmental pollution. They emit large amounts of greenhouse gases, such as carbon dioxide (CO2), which contribute to climate change. Additionally, they release other harmful pollutants such as sulfur dioxide (SO2), nitrogen oxides (NOx), and particulate matter (PM), which can cause respiratory problems, heart disease, and other health issues.

The environmental impact of thermal power plants is particularly acute in urban areas where they are located. The air pollution from these plants contributes to poor air quality and smog, which can have severe health consequences for people living in these areas. Furthermore, the discharge of untreated wastewater and cooling water from these power plants can also have significant environmental impacts, particularly on aquatic ecosystems.

The National Electric Power Regulatory Authority (NEPRA) of Pakistan regularly monitors the emissions from thermal power plants in the country. According to NEPRA's annual report for the fiscal year 2019-20, the Jamshoro Thermal Power Station emitted around 1.2 million tons of CO2 during that period. This is a significant amount of greenhouse gas emissions and highlights the environmental impact of thermal power plants in Pakistan.

		Furnace Oil	Natural Gas
(i).	SO_x (mg/Nm^3)	1550 to 1650	-
(ii).	NO_x (mg/Nm^3)	300 to 400	90 to 130
(iii).	CO_2 %	10.8 % to 14.0%	2.5 % to 2.7%

Fig. 3. Emission Values

NEPRA also reported that the air quality in the vicinity of thermal power plants was poor, with high concentrations of PM2.5 and PM10 (Particulate Matters). Additionally, the discharge of untreated wastewater and cooling water from these plants was also a concern, as it can impact the quality of water in nearby rivers and streams and is even more hazardous if the networks are near a residential area.

Environmental Impact of Steam and Coal Power Plants

Through its construction and operation, a power plant always affects our environment. As a power plant and its components take some space on the ground and in the air, it uses water resources and emits pollutants in many cases, which negatively impact our climate. Power plants emit air pollutants and water vapors, which affect the growth of certain crops. The plants are killed as some of the emitted pollutants are toxins or promote diseases.

Environmental Impact of Steam Power Plants

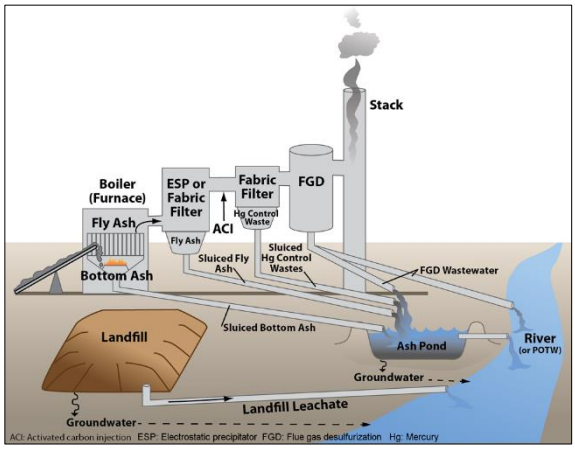

Fig. 4. Emission Values

According to the research, the impact of steam power plants on the environment is considered negative as we compare it to other energy sources. Steam power plants use three steam systems to generate electricity (nuclear power, coal power, and concentrated solar power), and each steam power system has a different impact on the environment. The steam system that has the mildest impact on the environment is the concentrated solar power system; it only affects our climate during its construction. Whereas nuclear power system has a negative impact on the environment due to the emission of carbon dioxide and other pollutants into the air.

There is a chance of catastrophic disaster while dealing with nuclear energy. Wastewater which contains large quantities of pollutants is discharged into the waters by steam power plants. The discharged pollutants sometimes include both toxic and bio accumulative pollutants, which include arsenic, lead, mercury, chromium, and selenium. Severe health and environmental problems are caused in the form of cancer and non-cancer risks in humans and lowered IQ among children. It not only affects humans but also causes deformities and reproductive harm in fish and wildlife. Many discharge pollutants remain in the environment for about three years, affecting our climate.

Environmental Impacts of Coal Power Plants

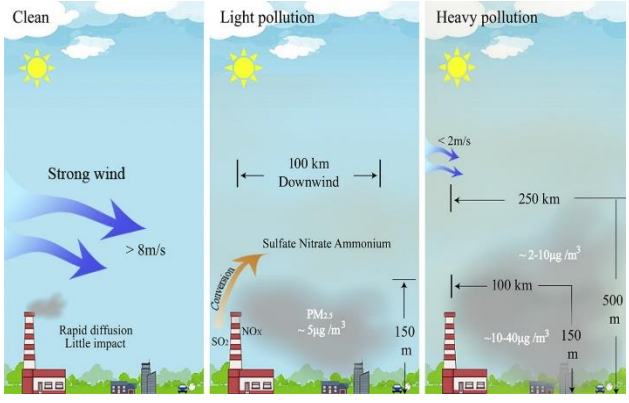

Fig. 5. Emission Values

When fossil fuels lie underground for thousands of years and heat and pressure are acted upon them, coal is formed, a carbon black rock that releases energy when burned. In Pakistan, coal is used by the power sector, and about 44.5% of the share has increased. About 61% of electricity comes from coal in Pakistan. In coal-fired power plants, steam is produced by burning fossil fuels to generate electricity and is considered to have the worst impact on the environment. Caron dioxide and other pollutants are released into the atmosphere as the burning of fossil fuels produces steam to generate electricity.

About 100 million tons of coal ash is produced by coal-fired power plants every year, and more than half of that waste ends up in rivers, lakes, ponds, and other sites, which with passing time, contaminate waterways and drinking water supplies. Pollutants from coal-fired plants lead to air pollution, which is linked to asthma, heart and lung ailments, cancer, acid rain, and other severe health impacts. Coal mostly consists of carbon, which produces carbon dioxide, a heat-trapping gas when burned in the air with oxygen. The most serious impact of the burning of coal on our environment leads to global warming.

Environmental Monitoring Report on Steam & Coal Power Plants

Air Quality:

The thermal and coal power stations emit pollutants such as particulate matter, sulfur dioxide (SO2), nitrogen oxides (NOx), and carbon monoxide (CO) into the atmosphere. The station uses flue gas desulfurization (FGD) technology to reduce SO2 emissions and low NOx burners to minimize NOx emissions. However, the emissions of particulate matter and CO can still have a significant impact on air quality. The concentration of particulate matter (PM10 and PM2.5) in the air surrounding the power station is higher than the national and international air quality standards.

Water Quality:

The Thermal & Coal Power Stations use water from the river for cooling and other processes. After treatment, the water is discharged back into the river to remove any pollutants. The water discharged from the power stations has to meet the national and international standards for pH, dissolved oxygen (DO), and the presence of heavy metals.

Soil Quality:

The emissions from the power station could impact soil quality, especially if the ash generated during coal combustion is not properly managed. The power station has measures in place to manage and dispose of the ash generated during combustion. The ash is transported to a nearby disposal site and is covered with soil to prevent it from being carried away by the wind. The ash disposal site does not have any impact on the surrounding soil quality.

Efficiency Of Thermal Power Plant Vs. Coal Power Plant

Thermal power plant	Coal Power Plant
• The overall efficiency of a thermal power plant is typically high, around 35% to 49%. • The efficiency of a thermal power plant depends on various factors, including the type of fuel used, the age of the plant, and the technology used. • Thermal power plants can use a variety of fuels, including coal, natural gas, and oil. • The efficiency of a thermal power plant can be improved by using more advanced technologies, such as combined-cycle power plants. • Thermal power plants require a steady supply of fuel to maintain their efficiency.	• The overall efficiency of a coal-fired power plant is typically lower than that of a thermal power plant, usually around 33%. • The efficiency of a coal-fired power plant is affected by various factors, including the quality of coal used, the age of the plant, and the technology used. • Coal-fired power plants require a steady supply of coal to maintain their efficiency. • The efficiency of a coal-fired power plant can be improved by using advanced technologies such as ultra-supercritical technology. • Coal-fired power plants emit a large number of greenhouse gases and pollutants, which can negatively impact the environment and human health.

Table 1. Emission Values

Why Is Thermal Power Plant Better Than Coal-Fired Power Plant?

There are various reasons why thermal power plants are considered better than coal power plants. Some of the reasons are as follows:

- A thermal power plant can use various fuels such as natural gas, oil, biomass, and even municipal waste, whereas a coal-fired power plant is restricted to only one fuel source: coal.
- Depending on the type of fuel, a thermal power plant's emission of pollutants and greenhouse gases are low when compared with coal power plants, which can emit lower levels of pollutants and greenhouse gases compared to a coal-fired power plant.
- The most crucial reason a thermal power plant is better is due to efficiency. Thermal power plants have higher efficiencies than coal-fired power plants, which means less fuel usage for the same amount of generation.
- Coal-fired power plants use large amounts of water to generate steam for their turbines, whereas thermal power plants can use condensers that require significantly less water.

Energy Outlook in Pakistan in 2025 And Beyond

Pakistan is currently facing major financial crises due to a combination of factors, including a high trade deficit, low foreign exchange reserves, and rising public debt. In its energy sector, the country faces high circular debt and a shortage of electricity supply. Circular debt, which refers to the accumulation of unpaid bills and inter-corporate borrowing, has been a longstanding issue in the energy sector, with the government struggling to clear the debts owed to power producers and distributors. This has led to a shortage of electricity supply, which has significantly impacted the economy and the daily lives of citizens.

Energy Supply and Demand Situation in Pakistan:

Pakistan's energy sector has been facing significant challenges in recent years, including a widening gap between demand and supply, outdated infrastructure, and increasing reliance on imported fuel. These challenges have led to frequent power outages and load shedding, negatively impacting the country's economic growth and development. Demand for energy in Pakistan has steadily increased due to population growth, urbanization, and industrialization.

According to the World Bank, Pakistan's energy demand is projected to triple by 2050. The country's electricity demand alone is expected to increase by an average of 6.5% per year until 2030. However, Pakistan's energy supply has been unable to keep pace with this rising demand, resulting in a significant energy deficit.

Pakistan's primary sources of energy are oil, gas, and coal, with renewables accounting for a very small share of the energy mix. However, the country has been exploring renewable energy sources such as solar, wind, and hydropower to diversify its energy mix and reduce dependence on imported fuel. The country's energy infrastructure needs modernization and investment as the transmission and distribution system is outdated and prone to frequent breakdowns.

Trends in Energy Consumption and Production in Pakistan:

Pakistan is facing a severe energy crisis due to a lack of investment in the energy sector, inefficient energy use, and an over-reliance on fossil fuels. Pakistan's primary energy source is oil, followed by natural gas, coal, and hydroelectricity. However, the country has been facing challenges in meeting its energy needs, resulting in frequent power outages and load shedding. To address these challenges, the government of Pakistan has been taking steps to diversify the country's energy mix and increase its renewable energy capacity. In recent years, Pakistan has made significant progress in renewable energy production, with solar and wind power becoming increasingly important sources of energy.

In 2020, renewable energy sources contributed approximately 5% to Pakistan's energy mix, with hydroelectricity being the largest contributor at 30%. However, the government aims to increase the share of renewable energy to 30% by 2030. Pakistan has also been investing in the development of its coal reserves, particularly in the Thar region. The country has one of the largest coal reserves in the world, but the quality of the coal is relatively low, requiring significant investment in infrastructure for extraction and processing.

Future of Coal-fired Power plants and Thermal Power Plants:

Coal-fired Power Plants

Despite having huge amounts of coal reserves in Thar, Pakistan may need to import coal. One of the main reasons is that the coal found in Thar may not be suitable for power generation technologies, so importing coal of better coal is necessary. Another reason is importing coal will be cheaper and more efficient than developing the domestic coal industry.

Coal-fired power plants will likely continue to play a significant role in Pakistan's energy mix, along with the growing interest in renewable energy. In order to reduce the environmental impact of coal-fired power plants, the government is likely to focus on improving the efficiency and environmental performance of plants.

Thermal power plants:

Thermal power plants are a major component of Pakistan's energy mix, and their outlook in the coming years will depend on several factors, including government policies, investment, and technological advancements. Some general trends or projects that may follow through with the future in Pakistan in terms of its thermal power generation are as follows:

1. According to the Pakistan Energy Outlook 2021 by the International Energy Agency (IEA), Pakistan's electricity generation is expected to increase by around 50% by 2030.
2. The government has announced plans to shift towards cleaner energy sources, including renewable energy and liquefied natural gas (LNG), which may impact the demand for thermal power plants in the coming years.
3. The efficiency of the current thermal power plants in Pakistan is relatively low compared to international standards, while investments and upgrading these plants could improve their outlook in the future.
4. Technological advancements in Carbon Capture, Utilization, and Storage (CCUS) could help reduce the environmental impact of thermal power plants on the environment, making it a more favorable component in the energy mix in the future.

Sustainable Solutions

The challenges facing thermal and coal power stations in Pakistan have many sides and require a joint effort to address. The unavailability of fuel, particularly furnace oil, and the use of outdated technology are significant obstacles that need to be overcome to ensure reliable and sustainable energy production. To overcome these challenges, Pakistan needs to explore alternative energy sources and invest in upgrading the technology used in thermal power plants. This will require a significant investment in energy infrastructure, including adopting modern technologies, using more efficient fuels, and better operation and maintenance practices.

It is essential for Pakistan to address these challenges and develop a sustainable energy system that meets the

country's growing energy demands. This can happen in the following ways:

Water Conservation

Power plants consume a significant amount of water for cooling and other processes. Implementing water conservation measures such as recycling and reusing water can reduce water consumption and help reduce the environmental impact of power plant operations. Pipeline leakages of water should be taken care of, so no water gets wasted.

Carbon Capture and Storage (CCS)

It is a process that involves capturing carbon dioxide (CO2) emissions from power plants and storing them underground instead of releasing them into the atmosphere. The process involves three main steps: capture (capturing CO2 emissions from the plant), transport (transported to a storage site), and storage (stored in a storage site such as depleted oil and gas reservoirs).

3. Conclusion

In conclusion, Pakistan's inefficient and outdated thermal power plants pose a significant environmental risk, and their efficiency can be improved by using imported coal. While coal-fired power plants offer affordable and reliable energy, they also have a considerable environmental impact. It is crucial for the government and the public to work together to find effective solutions that balance economic growth with environmental protection. Regular environmental monitoring and cost-effective measures should be carried out regularly to improve the efficiency of both types of power plants and should also be prioritized to minimize the environmental impacts.

4. References

1. GoP. (2014). Government of Pakistan, Ministry of Finance. *Pakistan Economic Survey 2013-14 - Energy [PDF].* Retrieved from: https://www.finance.gov.pk/survey/chapter_22/PES14-ENERGY.pdf
2. Jamshoro Power Co Ltd. (2020). LAG-02 GL Jamshoro Power Generation 13-02-2020 Modification-III [PDF]. *National Electric Power Regulatory Authority (NEPRA)*. Retrieved from: https://nepra.org.pk/licensing/Licences/Generation.PDF
3. Jamshoro Power Company Limited. (2019). TRF-255 JPCL FPA Oct 2019 19-11-2019 [*PDF*]. National Electric Power Regulatory Authority (NEPRA). https://nepra.org.pk/tariff/Tariff/GENCOs/JPCL/2019/TRF-255%20JPCL%20FPA%20Oct%202019%2019-11-2019%2024679-83.PDF
4. Jamshoro Power Company Limited. (2022). TRF-255 JPCL FPA Sep 2022 21-10-2022 [PDF]. National Electric Power Regulatory Authority. https://nepra.org.pk/tariff/Tariff/GENCOs/JPCL/2022/TRF-255%20JPCL%20FPA%20Sep%202022%2021-10-2022%2020572-77.PDF
5. Jamshoro power station. (2023, March 14). *Global Energy Monitor,* . Retrieved 05:16, November, 18, 2022 from https://www.gem.wiki/w/index.php?title=Jamshoro_power_station&oldid=402103.
6. Katzman, K. (2021). Pakistan-U.S. Relations [PDF]. Congressional Research Service. https://sgp.fas.org/crs/misc/RL34746.pdf
7. NEPRA. (2020). National Electric Power Regulatory Authority, *State of Industry Report 2020 [PDF]*. https://nepra.org.pk/publications/State%20of%20Industry%20Reports/State%20of%20Industry%20Report%202020.pdf
8. "Oil- and Gas-Fired Plants in Pakistan". (2013, July 10). *Power Plants Around the World*. Archived from the original on 18 July 2009. Retrieved March 19, 2014, from https://web.archive.org/web/20090718110554/http://www.industcards.com:80/tf-pakistan.htm
9. Rehman, A., & Deyuan, Z. (2018). Pakistan's energy scenario: a forecast of commercial energy consumption and supply from different sources through 2030. *Energy, sustainability and society*, *8*, 1-5. https://doi.org/10.1186/s13705-018-0167-y
10. "WAPDA Jamshoro Thermal Power Station". *Global Energy Observatory*. Retrieved March 23, 2014, from http://globalenergyobservatory.org/geoid/43217
11. World Bank. (2020, November 9). A Renewable Energy Future for Pakistan's Power System. https://www.worldbank.org/en/news/feature/2020/11/09/a-renewable-energy-future-for-pakistans-power-system

Saturn Publications

Frontiers in Engineering Science and Technology 1(2022) 2235-2241

www.saturnpublications/fest

Effect of Matrix Acidizing on Different Core Samples at Different Temperatures: An Experimental Study

Waseem Ali Shar[1,*], Syed Muhammad Usama[2], Waseem Ahmed[3], Jamshed Ahmed[4], and Zahir Khattak[5]

Dawood University of Engineering & Technology, Karachi, Pakistan

Received 15 June 2022; Accepted 23 September 2022

Abstract

The economic production of hydrocarbons from reservoirs is reliant on the natural capability of the reservoir to produce fluids (HCs) economically. However, a decrease in porosity, permeability, or both, can lead to damage near the wellbore face or deep into the rock, resulting in positive skin and resistance to fluid flow. This resistance causes a loss in production, which can be overcome by removing the impairments near the wellbore using stimulation methods. Matrix acidizing is a type of stimulation method that involves injecting an acid/solvent into the formation to dissolve/disperse materials that impair well production in sandstone reservoirs or to create new, unimpaired flow channels in carbonate reservoirs. The main aim of this study is to investigate and compare the effect of matrix acidizing on different rock formations at different temperatures, as well as to measure rock physical porosities (porosity, permeability) before and after acidizing. For this purpose, laboratory experiments were conducted on limestone (Tiyon formation) and sandstone (Gaj formation) of Thano Bulla Khan, Sindh, Pakistan. The experiments were conducted in two phases: pre-investigation of core samples and post-investigation of core samples. In the pre-investigation phase, experiments were performed before acidizing. These experiments included porosity, permeability, XRD, SEM, and EDS testing. In the post-investigation phase, experiments were performed after acidizing, except for XRD and EDS testing, which was only used for acid selection. The purpose of the post-investigation phase was to compare the results with the pre-investigation phase. Three samples of each formation were used to compare the results after injecting an acid combination (30-50ml) with a ratio of 15%HCL: 9% HCOOH, 13% CH3COOH at 60°C, 90°C, and 120°C. The results of the study showed that the effect of matrix acidizing was greater on limestone rock samples than on sandstone rock samples. Limestone rock is composed of calcium carbonate, which reacts vigorously with acid, while sandstone forms fewer bubbles. The petrophysical properties of the rock were successfully restored and recovered by doing the matrix acidizing job. In limestone rock samples, porosity values were recovered to 20.27% -23.18%%, and permeability values were recovered to 19.26 md to 24.16, 25.02, and 27.98 millidarcies at temperatures of 60°C, 90°C, and 120°C, respectively. In sandstone rock samples, porosity values were recovered to 7.5.

Keywords: Matric Acidizing; Rock Formations; Limestone Rock; Sandstone Rock; Carbonate Reservoirs.

1. Introduction

The oil and gas industries are heading towards the enhancement of recovery from low-permeable hydrocarbon reservoirs. The drilling, completion, and production activities of hydrocarbon reservoirs are the major reasons for formation damage. Due to this, damaging loss in production occurs. This can be achieved by stimulation methods by removing any disfigurement from the near wellbore. A well injection known as "well stimulation" is carried out on an oil or gas well to improve the flow of hydrocarbons from the drainage area into the well bore, increasing production. A matrix treatment increases production in both sandstone and carbonate wells by improving permeability by reducing damage near the wellbore. Although sandstone and carbonate use different acid systems, the same procedures apply to both. In the absence of damage, the significant amount of acid needed to raise permeability around the wellbore may not be warranted the little incremental improvement in output, particularly in sandstone. Hydrochloric acid tends to generate wormholes in carbonate rock, enlarging the wellbore or causing damage to be avoided. The increase in permeability is significantly greater in carbonate than in sandstone.

Well Stimulation

Stimulation is used to boost or recover a well's production. Sometimes a well initially shows limited permeability, in which case stimulation is used to start production from the reservoir. Sometimes stimulation is utilized to increase permeability and flow further from a well that already exists but has started to produce poorly.

*Corresponding author

The condition of the region surrounding the wellbore is one of the major constraints on establishing well productivity. By the value of "skin," all modifications to the initial construction are identified. The creation of the volume of rock with a reduced permeability in the vicinity of the wellbore region is correlated with formation damage. There are several causes for this decrease in permeability, but in every instance, it will lower "natural" production since there will be greater pressure decreases as the fluid gets closer to the wellbore.

A well's productivity can be increased by limiting the impact of formation damage in the vicinity of the wellbore or by putting a highly conductive structure on the formation. The two of the most generally used methods of well stimulation are:

- Acidizing
- Hydraulic Fracturing

Acidizing

The treatment of acidizing, a type of stimulation procedure, is carried out at a lower pressure than the reservoir fracture pressure in order to restore the naturally occurring permeability of the reservoir rock. Calcite, limestone, and dolomite cement are distributed throughout the sedimentary particles of the reservoir rocks by pumping acid into the well to produce well acidization. The use of matrix acidizing, and fracture acidizing are the two forms of acid treatment that are used.

Pumping acid into the well and the formation's pore throat enacts a matrix acidizing procedure. In this process of acidizing, the acids dissolve the mud particles and sediments while also enhancing the flow of hydrocarbons, decreasing the formation's permeability, and widening its pore throats. Fracture acidizing requires injecting high-pressure acid into the well, physically fracturing the reservoir rock, and dissolving the permeability blocking sediments. Matrix acidizing is carried out at a low enough pressure to prevent fracturing the reservoir rock. This kind of acid work creates routes for the hydrocarbons to move through.

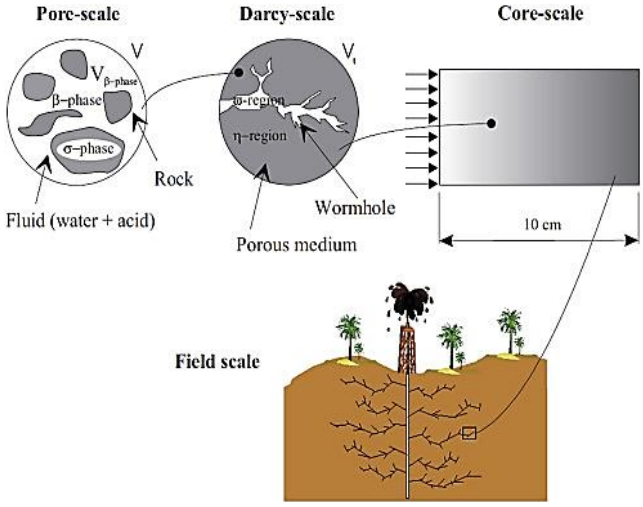

Fig. 1. Matrix Acidizing

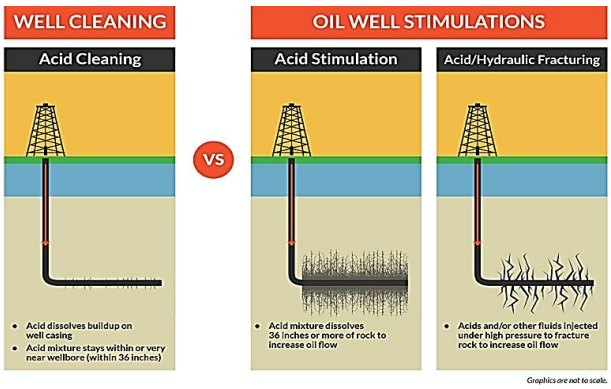

Fig. 2. Acidizing

Hydraulic Fracturing

Hydraulic fracturing is the stimulation method used by the petroleum industry the most frequently nowadays. Though educated estimations may reveal a discrepancy, the anemic claim that more than 70% of wells in North America have been fractured seems unconvincing. More than 3000 treatments have been given each month since 1955, on average. Hydraulic fracturing, which uses either acids or proppants to keep the crack open, is now the go-to method for the prompt. Acids or prop-pants fracturing is a good way to increase output in various areas. Many of the looming requirements for fracturing stimulation are formation-related, such as the uncertainty of whether the crack will spread over many formations and may interact with unwelcome water.

The four steps of the hydraulic fracturing process are as follows:

- A well is bored vertically to the desired depth, then is twisted at an angle, and continues parallel to the ground for thousands of feet into the formation thought to contain the trapped natural gas or oil.
- Natural gas or oil is released via the cracks and is brought back up the well to the surface after being pushed through a high-pressure mixture of water, sand, and chemicals into the well in order to form fissures in the shale rock.
- Following the fracturing procedure, wastewater, often known as "flow back water" or "generated water," rises to the surface.
- The oil or natural gas is gathered at the surface and is processed, refined, and shipped to the market.

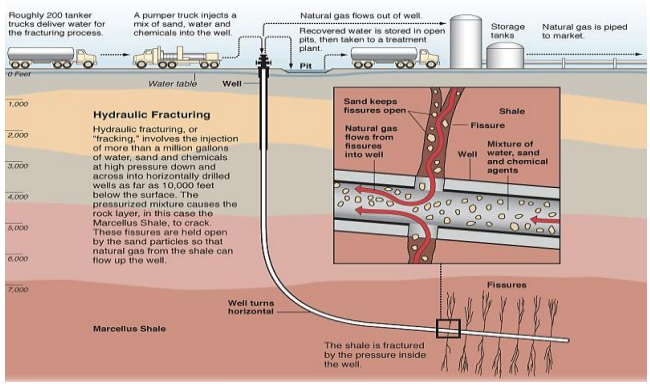

Fig. 3. Hydraulic Fracturing

Matrix Stimulation

To dissolve or scatter contaminants that hinder well production in sandstone reservoirs or to establish new, unhindered flow channels in carbonate reservoirs, matrix stimulation involves pumping an acid or solvent into the formation at a pressure lower than the formation's fracture pressure. Since mineral acids are most typically utilized in matrix stimulation, this process is also sometimes referred to as "matrix acidizing." When matrix acidizing, all the acid reacts in carbonates within a few to maybe as much as 10 feet of the wellbore. For oil wells, the lower permeability limit for matrix acidization is 10mD, and for gas wells, it is 1mD. Only a small portion of the matrix in sandstone is soluble, therefore the permeability-damaging minerals are dissolved by relatively slow-acting acid.

A/c to the thumb's rule, matrix acidizing is only used when a well has a significant skin impact that cannot be attributable to operational, surface or mechanical issues. Before attempting to remove damage by matrix acidizing, the kind (or Cause) and location of the damage must be determined. The damage identification process involves:

- Examining the well records to identify operations that might have resulted in formation damage
- Carrying out specific laboratory testing, such as a reservoir core flushing, to determine if the identified operations did indeed lead to core damage for the particular combination of the fluids in question and the reservoir formation
- Examining the damaged core with sophisticated analytical techniques such as the scanning electron microscope to confirm the damage type and location and develop ideas on how to remove it.

2. Problem Statement

When a reduction occurs in the natural capability of a reservoir to produce its fluids (HCs) economically, such as a decrease in porosity or permeability, or both, damages can occur near the wellbore face or deep into the rock. It shows that skin is damaged, either it is positive or negative, which causes the resistance to fluid flow around the wellbore or in the reservoir. Most of the hydrocarbon generating formations has been damaged, whether by drilling, completion, and production activities. This can be achieved by removing any impairment from close to the wellbore by the stimulation methods. This damage is caused by several mechanisms:

- Physical plugging of pores by mud solids
- Alteration of reservoir rock wettability
- Precipitation of insoluble materials in pore spaces
- Clay swelling in pore spaces.
- Migration of fines into pore throats
- Introduction of an immobile phase
- Emulsion formation and blockage

To remove damage near the well bore, matrix acidizing is done to eradicate this, but due to the temperature of the reservoir, it causes an unstable effect of acid in the form of precipitation, reaction with minerals, or corrosion problems.

3. Objectives of the Study

The objectives of the project are:

1. Study the effect of matrix acidizing before and after acidizing on different rock samples at different temperatures.
2. Evaluate porosity and permeability before and after acidizing.
3. Compare the results of each other before and after acidizing to differentiate the effect of matrix acidizing on them.

4. Scope of the Study

By removing damaged or creating new channels, acidizing sandstone, and limestone reservoirs is a crucial step to ensuring high output. Numerous studies have been conducted to date emphasizing the value of acidizing sandstone formations. Many researchers developed different acid combinations, and applied different chelating agents to get the best results related to

- Permeability
- Porosity
- Precipitation

Due to the limitations of the current acid combinations at high-temperature wells and the limited research on these combinations on various sandstone and limestone formations, new acid combinations are needed for future sandstone and limestone acidizing aspects, and more research is required on the current technology.

Future research should focus on creating acid mixtures that may be used effectively to reduce the problem of precipitation reaction at high temperatures. Future research on the effects of acidizing on the topology, morphology, and wettability of rock samples would greatly benefit from pore-scale imaging.

5. Literature Review

In order to properly select stimulation candidate wells, it is necessary to first have an in-depth understanding of the concepts of formation damage and well stimulation. A lot of research conducted on formation damage and well stimulation methods can be found in the literatures. Well stimulation is considered a major key to proper reservoir management; hence several authors made valid contributions.

Guo et al. (2020) took four core samples from the Eagle Ford shale formation, measuring 3.81 cm in diameter and 15.24 cm in length, and were experimentally evaluated to determine how matrix acidizing affected them. The average mineralogical compositions of the core samples were constituted by calcite (48.8%), siderite (18.1%), and dolomite (11.9%). At room temperature and atmospheric pressure, the samples were in 15% HCl for 24 hours. According to the research, the acid dissolved an average of 38% of the core samples, increasing their true porosities.

Sheng et al. (2019) using a 15% HCl and 3% KCl acid combination for 10 hours, researchers in China examined the effects of acidizing treatments on two different types of core samples from the Longmaxi marine and Yanchang

continental shale formations. Compared to the clay contents, which were 27% and 26% for the core samples from Longmaxi and Yanchang, respectively, the carbonate concentrations were 18% and 4%. Each core sample was dipped in 5 cm3 of the acid mixture for two hours before being left to dry naturally for 24 hours at room temperature (26 °C). According to the observations, carbonate minerals were dissolved by the acid, which allowed cracks to form and the pore spaces to connect. These minerals include carbonates, anhydrite, and clay, and as a result of this process, the produced tensile stress and increased the porosities of the samples.

Weldu Teklu et al. (2019) examined the effects of 1 and 3% HCl dissolved in 10% KCl (potassium chloride) brine on the porosity and permeability of 48 Canadian shale core samples from the Otter Park (14 samples), Muskwa (23 samples), and Evie (11 samples) formations. The top and bottom surfaces of the core samples were in contact with 1 or 3% HCl acid (three times the rock mass) at room temperature for four days after being covered with tape. According to the findings, HCl improved the core samples' porosity and permeability.

Wu and Sharma (2017) Studied the matrix acidizing on a single undamaged Bakken shale core. According to the XRD test results, 24% of the core sample was quartz and 27% was calcite. 50 mL of 3% HCl and 3% KCl were used to dissolve around 35% of the Bakken powder sample. The shale sample's microstructure, pore structure, and material properties were all altered by the acid. Minerals that are structurally stable in acidizing processes include clay, quartz, and organic materials. However, if the near carbonates break down in HCl, they can be removed. Acidification produced macro pores with a 120 μ(m) diameter that decreased the hardness of the shale fracture surface by 30–70% and improved fracture conductivity. The outcome was an increase in permeability and porosity, which may increase the hydrocarbon flow.

According to Khalil et al. (2017); and Khalil et al. (2020), the reservoir rock is far less permeable than the conductive flow channels (wormholes) made by matrix acidizing. As a result, near-wellbore damage and poor permeability zones can be easily overcome by fluid movement through these wormholes from the formation into the wellbore. This experimental investigation showed that performing matrix acidizing with 15% HCl on Eagle Ford core samples (a carbonate-rich shale formation) significantly increases the permeability of the core samples (from nanodarcies to microdarcies).

Zhou et al. (2016) performed core flooding tests at 25 and 65 °C with 12% HBF4 and 12% HCl. The outcomes were contrasted with those of standard 3% HF and 12% HCl. According to the findings, the fluoroboric acid combination exhibits a 40% greater permeability enhancement than the typical mud acid. Additionally, at 65 °C, permeability enhancement is larger than at 25 °C. The research solely examined the differences between 25 °C and 65 °C.

Schmid et al. (2016) asserted that an engineer must consider all relevant data during a matrix acidizing operation, including well history, laboratory test results, and previous operation experience, in order to choose the acidizing treatment fluid. A thorough reservoir characterization workflow method is necessary to guarantee the success of a matrix acidizing treatment. Abdelmoneim & Nasr-El-Din (2015) found the ideal HF concentration for formations of high-temperature sandstone. The core flooding tests on the Grey Berea core and Bandera core were carried out at high temperatures of 280 and 325 °F. The association between the ideal HF concentration and mineralogy was established as an inverse relationship as a result of the findings.

Similarly, Tripathi and Pournik (2014) experimentally examined the impact of matrix acidizing on four core samples from the Eagle Ford shale formation, measuring 3.81 cm in diameter and 15.24 cm in length. The majority of the core samples' average mineralogical compositions were calcite (48.8%), siderite (18.1%), and dolomite (11.9%). The samples were placed in 15% HCl for 24 hours at ambient temperature and atmospheric pressure. The research indicates that an average of 38% of the core samples were dissolved by the acid, increasing their actual porosities.

Morsy et al. (2013) gathered shale samples from Eagle Ford, Mancos, Barnett, and Marcellus. Shale formations were examined for the effects of hydrochloric acid (HCl) on porosity, sudden solubilization, and fracture spread. In that investigation, several acid concentrations of 4, 15, and 20% were examined. The results showed that the best acid concentration for increasing porosity and oil recovery without destroying the structures of the core samples was 4% HCl. Additionally, they suggested using low-concentration HCl inside the shale formation as well as around the wellbore as part of the hydraulic fracturing procedure.

Gomaa et al. (2013) stated that the change in permeability of the sandstone core matrix at a temperature of 180 °F was examined in relation to the ratio of mud acid content. There are four different mud acid concentration ratio mixtures: 1.9% HF+15% HCl, 2.3% HF+10% HCl, 2.6% HF+5% HCl, and 2.8% HF+3% HCl, respectively. The core flooding technique was used to examine each of them utilizing a core sample. According to the experimental findings, the permeability of the core sample can be positively increased by all four acid mixing ratios. However, it was found that as the HF-HCl ratio rises, the permeability result increases.

Parkinson et al. (2010) applied a different strategy to enhance the Pinda formation's production zone, which is in West Africa. The Pinda formation contained many carbonate layers. This formation's BHST (bottom hole static temperature) was 300 °F. During the main flush stage, a PH 4 HEDTA chelant was used to stimulate the six production wells from the formation zone. The outcome revealed that all six wells are now producing at a rate that has doubled since the stimulation, demonstrating a strong economic return from the high temperature stimulating acid.

Whereas. Jaramillo et al. (2010) indicated that by combining organic acid and HBF4 to create a new acid system known as organic clay acid, it was possible to further develop the use of HBF4 acid in the acidification of

sandstone (OCA). Many wells had been treated in low-temperature reservoirs at less than 140 °F after being stimulated with OCA. The efficiency of OCA in particle management and clay stability was demonstrated by actual field findings. It had been noted that the initial production rise on the wells stimulated with OCA was greater than the initial production increase on the wells treated with organic mud acid. This demonstrated that OCA had successfully stopped the fines migration problem produced by organic mud acid.

In a study, Ali et al. (2008), using an experimental technique, discovered that sodium hydroxyethylethylenediaminetriacetic acid (Na3HEDTA), a low-pH solution, can promote the development of high-temperature fluids in West Africa. The outcome showed that the chelating fluid is effective in raising the high-temperature well's permeability. Further, Frenier et al. (2004) found that hydrox-ethylaminocarboxylic acid (HACA)-based chelate was created and tested on Berea sandstone. The outcomes showed that the high-temperature sandstone reservoir could employ this HACA chelate.

Thomas et al. (2001) performed core flooding on Jauf core samples using HCl and acetic acid in the pre-flush at 150 °C. The channels made by the pre-flush acid, which was utilized before the mud acid, were important since they showed up in the results. The permeability had been greatly improved by channeling effects during the main acid application.

Similarly, Van Domelen and Jennings (1995) ascertain that due to the fact that it produces no insoluble products from interactions with minerals, HCl plays an important role in mud acid. Along with being advantageous in terms of cost, HCl has been used extensively for sandstone stimulation. Additionally, and especially in high temperature, high-pressure (HTHP) formation environments, HCl is extremely corrosive and dangerous to the well.

Ayorinde et al. (1992) demonstrated the benefit of HBF4 in treating an oil well in Nigeria that had had serious fines migration-related problems brought on by traditional mud acid. HBF4 had indicated compatibility with fines migration stabilizing. 850 barrels of liquid are produced by the oil well per day after it has been acidified with mud acid (BLPD). However, because to fines migration, production decreased to almost nothing. Following a successful HBF4 treatment, production rose to 2500 BLPD and remained constant at 220 barrels of oil per day (BOPD) even after a year.

6. Methods

Area of Study

Our research study is based on rocks of two different formations, limestone is from the Tiyon formation, and sandstone is from the Gaj formation. Both formations belong to Thano Bulla Khan. It is located at 25°24'34.9"N 67°46'27.1"E Jamshoro, Sindh, Pakistan. The main terrain of the region is made up of hills and valleys that alternate, with their long axes running north to south. The region's geology is made up of marine-derived sedimentary formations as well as certain volcanic sills, which are injected with igneous bodies horizontally. With geological ages ranging from recent to Cretaceous, lithology materials such as sand, clay, silt, gravel, limestone, conglomerate, sandstone, and shale are discovered. The area is complicated structurally because beds exhibit severe dips, main structure limbs either have opposing inclinations or show dipping in the direction of one another, and thrust faulting, synclines, and anticlines are all clearly apparent. The valley is covered with substantial amounts of alluvium, which includes sand, silt, clay, and gravel. In the display, the region's geology is described.

Collection and Cutting of Rock

We have collected two surface rock samples (limestone and sandstone) from Thano Bulla khan Jamshoro, Sindh, Pakistan. Limestone from the Tiyon formation and sandstone from the Gaj formation. After collecting rock samples, Cut the rock samples into a finely cylindrical shape by using a drill press (3 samples of each rock with the core length of 1.5 inches and diameter of 1 inch).

Preparation of Core Samples

First of all, we arranged two different rock samples, i.e., limestone and sandstone, for the matrix acidizing job and then cut them into small core samples in a fine cylindrical shape by using the drill press to perform acidizing experiment on it. Cut in a way the size of samples should be equal. We took all samples to the laboratory and ensured samples were clean and under the same conditions at room temperature and pressure. We use three small core samples (1.5 inches) of limestone and three small (1.5 inches) core samples of sandstone.

Pre-Investigation of Core Samples

After cutting rock samples, the core samples are further treated in the laboratory for pre-investigation of core plugs. In this phase, we did five tests for all given samples.

i. XRD (X-ray Diffraction)
ii. SEM (Scanning Electron Microscopy)
iii. EDS (Energy Dispersive X-ray Spectrometry)
iv. Porosity measurement
v. Permeability measurement

Post Investigation of Core Samples

After Acid Preparation, the core samples are further treated in the laboratory for Post investigation of core plugs/samples. In this phase, we inject a combination of acids into core samples by using a syringe at different temperatures (60°C,90°C,120°C), and then we go for post-investigation and do three tests for all given samples.

i. SEM (Scanning Electron Microscopy)
ii. Porosity measurement
iii. Permeability measurement

7. Results and Comparison

Throughout the project, we have done many experiments and laboratory testing to investigate and compare the effect

of matrix acidizing before and after acidizing on different core samples at different temperatures and found the following results.

Name of samples	Before Acidizing		After Acidizing			
	Porosity (%)	Permeability (md)	Porosity (%)	Permeability (md)		
				60°C	90°C	120°C
Limestone	20.27	19.26	23.18	24.16	25.02	27.98
Sandstone	7.5	14.82	9.47	19.68	19.45	20.22

Table 1. Comparative Chart of Porosity and Permeability of Sandstone before and After Acidizing

Our basic objectives were to increase porosity and permeability. We prepared acid combination by analyzing XRD and EDS testing and found the following:

- Limestone is mostly composed of calcite and magnesium minerals with a percentage of 69.29%, and the shape of the crystal is rhombohedral.
- And sandstone is mostly composed of calcite magnesium (74%) and dolomite (24%) minerals, and the shape of the crystal is rhombohedral.

After we performed the matrix acidizing job on samples and found the expected results as

- The initial average porosity of limestone and sandstone was 20.27% and 7.5%, respectively, and after acidizing job, it increased with the percentage of 3% and 2%, respectively, compared to its initial value, which is quite better.
- The initial permeability of the limestone was 19.26 md, and after acidizing job, we found that permeability increases as temperature increases. final permeability of limestone at 60°C, 90°C, and 120°C is 24.16, 25.05, and 27.98 md respectively.
- Similarly, the initial permeability of sandstone was 14.82, whereas the final permeability was 19.68, 19.45, and 20.22 md at temperatures 60°C, 90°C, & 120°C, respectively.
- Comparative graphs of porosity and permeability are given below.

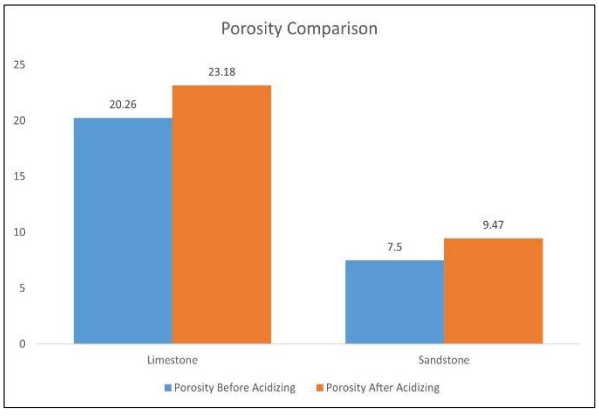

Fig. 4. Comparative Graph for Porosity

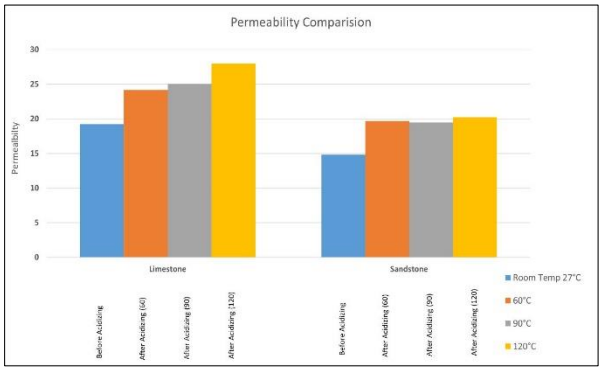

Fig. 5. Comparative Graph Permeability

8. Conclusion

Our main objectives were to increase the porosity and permeability of the reservoir after acidizing on different core samples at different temperatures.

- It is concluded that this acid combination gives the best results in limestone formation at high temperatures as it increases porosity and permeability up to 25% and 30%, respectively.
- The result is clearly seen that acid has reacted more effectively with limestone rock samples than with sandstone.
- The acid dissolves minerals, and no corrosion problems occur in limestone.
- While this acid combination is not recommended for sandstone formation due to precipitation which can block perforations and pore throat, this research provides strong evidence and complement. The methodology we use will help for the modern application in production engineering as well as it helps to explore a greatly enriched area in hydrocarbons.
- We must enhance the fieldwork for development, which is heavily focused on observing and interpreting the geological information present in the outcrop of Thano Bulla Khan.
- This project recommends upcoming changes and challenges in the domain of matrix acidizing and their performance for porosity and permeability increase (wormhole effect).

9. References

1. Abdelmoneim, S. S., & Nasr-El-Din, H. A. (2015, June). Determining the optimum HF concentration for stimulation of high-temperature sandstone formations. In *SPE European Formation Damage Conference and Exhibition*. OnePetro.
2. Ali, S., Ermel, E., Clarke, J., Fuller, M. J., Xiao, Z., & Malone, B. (2008). Stimulation of high-temperature sandstone formations from West Africa with chelating agent-based fluids. *SPE Production & Operations*, *23*(01), 32-38.

3. Ayorinde, A., Granger, C., & Thomas, R. L. (1992). The application of fluoboric acid in sandstone matrix acidizing: a case study.
4. Frenier, W., Brady, M., Al-Harthy, S., Arangath, R., Chan, K. S., Flamant, N., & Samuel, M. (2004, February). Hot oil and gas wells can be stimulated without acids. In *SPE International Symposium and Exhibition on Formation Damage Control*. OnePetro.
5. Gomaa, A. M., Cutler, J., Qu, Q., Boles, J., & Wang, X. (2013, June). An effective single-stage acid system for sandstone formations. In *SPE European Formation Damage Conference & Exhibition*. OnePetro.
6. Guo, J., Gou, B., Qin, N., Zhao, J., Wu, L., Wang, K., & Ren, J. (2020). An innovative concept on deep carbonate reservoir stimulation: three-dimensional acid fracturing technology. *Natural Gas Industry B*, *7*(5), 484-497.
7. Jaramillo, O. J., Romero, R., Ortega, A., Milne, A., & Lastre, M. (2010, February). Matrix acid systems for formations with high clay content. In *SPE International Symposium and Exhibition on Formation Damage Control*. OnePetro.
8. Khalil, R. E., Emadi, H., & Gamadi, T. (2020, June). An experimental investigation analyzing effects of injection pressure on efficiency of matrix acidizing stimulation on Marcellus shale core samples. In *54th US Rock Mechanics/Geomechanics Symposium*. OnePetro.
9. Khalil, R. E., Mansour, A., & Gamadi, T. (2017, September). An experimental study of acid matrix treatment performance on shale core samples. In *SPE Liquids-Rich Basins Conference-North America*. OnePetro. https://doi.org/10.2118/187478-MS
10. Morsy, S., Sheng, J. J., & Soliman, M. Y. (2013, August). Improving hydraulic fracturing of shale formations by acidizing. In *SPE Eastern Regional Meeting*. OnePetro.
11. Parkinson, M., Munk, T., Brookley, J., Caetano, A., Albuquerque, M., Cohen, D., & Reekie, M. (2010, February). Stimulation of multilayered high-carbonate-content sandstone formations in West Africa using chelant-based fluids and mechanical diversion. In *SPE International Symposium and Exhibition on Formation Damage Control*. OnePetro.
12. Schmid, W., Martin, A., & Palacios, J. M. (2016, June). Comprehensive approach of reservoir characterization has allowed successful stimulation of sandstone formations in Bachaquero Field-Lake Maracaibo, Venezuela. In *SPE Trinidad and Tobago Section Energy Resources Conference*. OnePetro.
13. Sheng, G., Su, Y., & Wang, W. (2019). A new fractal approach for describing induced-fracture porosity/permeability/compressibility in stimulated unconventional reservoirs. *Journal of Petroleum Science and Engineering*, *179*, 855-866.
14. Thomas, R. L., Nasr-El-Din, H. A., Lynn, J. D., Mehta, S., & Zaidi, S. R. (2001, September). Precipitation during the acidizing of a HT/HP illitic sandstone reservoir in eastern Saudi Arabia: a laboratory study. In *SPE Annual Technical Conference and Exhibition*. OnePetro.
15. Tripathi, D., & Pournik, M. (2014, August). Effect of acid on productivity of fractured shale reservoirs. In *SPE/AAPG/SEG Unconventional Resources Technology Conference*. OnePetro.
16. Van Domelen, M. S., & Jennings, A. R. (1995, September). Alternate acid blends for HPHT applications. In *SPE Offshore Europe*. OnePetro.
17. Weldu Teklu, T., Park, D., Jung, H., Amini, K., & Abass, H. (2019). Effect of dilute acid on hydraulic fracturing of carbonate-rich shales: experimental study. *SPE Production & Operations*, *34*(01), 170-184.
18. Wu, W., & Sharma, M. M. (2017). Acid fracturing in shales: effect of dilute acid on properties and pore structure of shale. *SPE Production & Operations*, *32*(01), 51-63.
19. Zhou, X., Zhang, S., Zhang, X., Wang, F., & Lin, H. (2016). Core-Scale Experimental and Numerical Investigation on Fluoroboric Acidizing of a Sandstone Reservoir. *Energy Technology*, *4*(7), 870-879.